The protein interactome of the citrus Huanglongbing pathogen *Candidatus* Liberibacter asiaticus

Erica W. Carter[1, 2], Orlene Guerra Peraza[1], and Nian Wang[1,3]*

[1]Citrus Research and Education Center, Institute of Food and Agricultural Sciences, University of Florida, Lake Alfred, FL, USA.

[2] Department of Plant Pathology, Institute of Food and Agricultural Sciences, University of Florida, Lake Alfred, FL, USA.

[3]Department of Microbiology and Cell Science, Institute of Food and Agricultural Sciences, University of Florida, Lake Alfred, FL, United States.

*Corresponding author email: nianwang@ufl.edu

Abstract

Candidatus Liberibacter asiaticus (CLas) is the causal agent of the devastating citrus Huanglongbing (HLB) disease. Our understanding of the pathogenicity mechanism and biology of CLas remain limited because CLas has not been cultured in artificial media. CLas encodes 1136 proteins of which 415 have unknown functions. Since genetic studies of CLas genes with unknown functions are impossible, we utilized genome-wide protein-protein interactions (PPIs) yeast-two-hybrid (Y2H) assays to help solve the mystery. PPIs are fundamental to all cellular processes and machinery and instrumental in investigating uncharacterized proteins and inferring biological pathways. In total, 916 bait and 936 prey proteins were included in the three-phase screening, which identified 4245 interactions. The false positive rate of the Y2H assay was estimated to be 3.1%. Pull-down assays confirmed the robustness of our Y2H. The average interactions per node for CLas Y2H interactome were approximately 15.6, significantly higher than free-living bacteria, indicating genome reduction has led to a multi-function of proteins. PPIs provide clues for functions of 371 uncharacterized proteins of CLas. Forty HUB node proteins were identified which might play critical roles in CLas, including a quinone oxidoreductase and LysR that are known to protect bacteria against oxidative stress. This explains why CLas survives well in the phloem even though it triggers immune-mediated disease, systemic and chronic production of reactive oxygen species, and phloem cell death. This PPI database facilitates the investigation of CLas cellular biochemistry and physiology, functions of uncharacterized proteins, and pathogenicity mechanisms of the pathogen.

Main

Citrus Huanglongbing (HLB) is one of the most destructive plant diseases worldwide, and no effective and economic disease control measures are available for HLB-endemic citrus production regions[1]. HLB has devastated the citrus industry in many regions, including Florida, US[2]. HLB is caused by *Candidatus* Liberibacter asiaticus (CLas), *Ca*. L. americanus, and *Ca*. L. africanus, with CLas being the most prevalent. *Ca*. Liberibacter species are endophytic bacteria that colonize the phloem tissues of citrus plants and are transmitted by the hemipteran insect *Diaphorina citri*[3,4]. The environments inside the phloem tissue and psyllids are nutrient rich. Consequently, *Ca*. Liberibacter species have undergone reductive evolution and have considerably smaller genomes (approximately 1.2 MB) than their culturable, free-living relatives, such as *Agrobacterium*[3,4]. Cultivation of HLB pathogens in artificial media has not been achieved despite extensive effort[5], which prevented genetic manipulation and impeded understanding of their biology and pathogenicity mechanism.

The CLas genome encodes approximately 1,027 proteins, of which 612 have predicated functions based on sequence similarities with characterized proteins from culturable microorganisms. However, 415 CLas proteins have no known functions[4]. Investigating protein functions, particularly those with unknown roles, is critical for elucidating the biology and pathogenicity of CLas and developing effective strategies to combat this notorious citrus disease. Protein–protein interactions (PPIs) are fundamental to all cellular processes and machinery. PPIs modify enzyme and protein activities, catalyze metabolic reactions, and activate signaling pathways[6]. Interactions with proteins of known functions provide informative clues for function prediction of uncharacterized proteins[7]. Exploring PPIs was also used to investigate biological pathways[8]. Furthermore, targeting PPIs can be used to develop novel antimicrobials[9]. The Yeast Two-hybrid system (Y2H) is the most commonly used approach to investigate interactomes and has been elegantly applied to various organisms, such as animals, *Drosophila melanogaster*[10] and *Caenorhabditis elegans*[11,12]; plants, *Arabidopsis thaliana*[13,14]; fungi, *Saccharomyces cerevisiae*[7]; and bacteria, *Streptococcus pneumoniae*[15], *Treponema pallidum*[16], *Campylobacter jejuni*[17], *Synechocystis sp.*[18], *Mycobacterium tuberculosis*[19], *Mesorhizobium loti*[20], *Escherichia coli*[21], *Bacillus subtilis*[22], and *Helicobacter pylori*[8,23]. Affinity Purification Mass Spectrometry (AP-MS) has also been used to study the *Mycoplasma pneumoniae* interactome[6,24] (Extended Data Table S1). However, AP-MS detects PPIs in the native organism, which prevents its application in non-cultured microorganisms such as CLas, whereas Y2H, using a non-native

host: yeast, bypasses this limitation. Interactome studies (Extended Data Table S1) have led to significant progress in inferring the function of unknown proteins, elucidating protein organization of a cell, identifying novel functions of known proteins, and in some cases, are used to find interaction points between pathogenic organisms and their eukaryotic hosts [25–31]. Here, we conducted a genome-wide Y2H interactome study of CLas.

High-throughput Y2H screening. We conducted Y2H assays to identify the CLas interactome. Full-length open reading frames (ORFs) were used for yeast vector construction to increase the possibility of identifying biologically relevant interactions. 974 ORFs were PCR amplified (Supplementary Dataset S1), and 942 ORFs were successfully cloned (Extended Data Figure S1A). In total, 926 "bait" proteins in pGEO_BD, which was modified from pGBKT7_BD (Extended Figure S1B), and 950 "prey" proteins in pGAD_T7 remained. After the removal of autoactivating constructs (Extended Data Figure S2), 916 "bait" and 936 "prey" constructs were used in the screening, representing 91% of genes encoded by CLas. We constructed the CLas binary interactome using a three-phase array screening method (Figure 1A). The first two pooled array phases removed non-interactors. Proteins interacting on the most stringent media, QX (-trp, -leu, -ade, -his, +XαGal) and QXA (-trp, -leu, -ade, -his, +XαGal, +AbA) in the first two screening phases were used in the pairwise array in the third screening phase. The pairwise screening enabled us to identify all potential interactions from the mini-pooled arrays and detect the interacting partners. In addition, pairwise rescreening eliminated probable promiscuous proteins from the dataset. The final (third phase) screening between 617 baits and 466 preys resulted in 4245 interactions between 542 proteins (Supplementary Dataset S2), covering 52.8% of CLas genes, denoted as the CLas_whole network (Figure 1B). Among the 542 proteins, 371 had known functions, whereas 171 were uncharacterized proteins (Supplementary Dataset S3; Extended Data Tables S2 and S3).

CLas interactome coverage and confidence scores. The robustness of the Y2H datasets is imperative for utilizing the PPI information [8,23,32–34]. We reduced false positives by pairwise rescreening and stringent selection of the CLas network in the three-phase screening. To evaluate the sensitivity and reproducibility of the three-phase method, we subjected a random set of 326 yeast constructs (163 proteins in each vector) to an independent pairwise Y2H screening. We observed 832 reproducible interactions between the three-phase and pairwise screening,

93 representing 92% of the interactions detected between those 163 proteins in the CLas_whole
94 network.

95 We further employed known PPIs in the STRING-db to evaluate the sensitivity of the two
96 screening assays. Limited information is available for CLas in the STRING database, with no
97 experimentally determined interactions reported for CLas specifically. However, there were 474
98 and 369 experimentally determined interactions between homologous proteins (iPPIs) and
99 interacting protein families interologs (iCOGs) at confidence cutoffs ⩾0.4 and ⩾0.9,
100 respectively (Extended Data Table S2; Table S4) [35,36]. Our results showed that both Y2H
101 screening methods had comparative sensitivity in detecting predicted CLas interactions based on
102 known PPIs of homolog proteins. Each CLas Y2H screening detected 41 of the 117 predicted
103 interactions among these 163 proteins (Figure 1C, Supplementary Dataset S4).

104 Using the interactions detected in the two Y2H screening methods, we calculated the false
105 positive rate for the high-throughput three-phase Y2H screening as 3.1% and the false negative
106 rate as 47.9%. Thus, our three-phase Y2H is stringent against false positives in identifying
107 putative PPIs of CLas. However, though the high throughput three-phase screening is efficient, it
108 also brings a significant trade-off of a false negative rate of 47.9%, probably resulting from the
109 pooling used in the 1st and 2nd phases. Nevertheless, the low false positive rate rendered our
110 three-phase Y2H data highly robust to analyze the CLas interactome and infer the protein
111 function of hypothetical proteins.

112 To evaluate the robustness of individual PPIs, we calculated interaction confidence scores for the
113 CLas_whole network PPIs using interologs as the positive reference set. The interologs were
114 obtained by querying the STRING-db for experimentally determined PPIs from *Agrobacterium*
115 *radiobacter, B. subtilis*, *C. jejuni*, *E. coli, H. pylori, L. crescens*, *M. genitalium*, *M. loti*, *M.*
116 *pneumoniae, S. cerevisiae, S. meliloti, T. pallidum,* and iCOGs. There were 635 interologs
117 between 208 protein pairs in the CLas_whole network. We used 100 PPIs corresponding to
118 interologs with the highest confidence scores representing the positive reference set for logistic
119 regression analysis to assign interaction confidence scores to CLas_whole PPIs (Supplementary
120 Datasets S5 and S6). In total, 2314 interactions between 455 proteins demonstrated high
121 confidence scores (⩾0.5, CLAS_HC), representing 55% of the total interactions detected in the
122 CLas_whole network and 44% of the CLas ORFs (Figures 1B & 1D, Supplementary Dataset S7)

123 To further verify our Y2H PPIs, we conducted pull-down assays for nine PPIs focusing on
124 flagellar proteins because of the crucial roles of CLas motility in the HLB pathosystem [37].
125 Consistent with the Y2H result, nine tested PPIs were confirmed (Figure 2), supporting the high
126 quality of the three-phase Y2H screening.

127 **Network Topology.** Protein network topology provides valuable information for protein
128 functions[38,39]. We visualized and analyzed the topology of the CLas Y2H interactome (Figure
129 3A-C)[40,41]. The degree distribution topology of CLas_whole had a scale-free organization,
130 typical of a scale-free PPI network (Figure 3D)[27]. The average number of interactions per node
131 was 15.664 in the CLas_whole network; CLas_HC has an average node degree of 10.171. The
132 CLas network had many node neighbors, consistent with the notion that protein function
133 complexity increases with genome reduction (Figure 3F, Extended Data Figure S3) [6,42,43]. The
134 CLas_HC network maintained a degree distribution and topological coefficient distribution like
135 that of the CLas_whole network (Figures 3D and G). However, the clustering coefficient and
136 betweenness centrality distribution of CLas_HC were less dense than the CLas_whole with
137 fewer crosstalk between nodes (Figures 3E and F)[6].

138 Highly connected nodes (HUBs) are more likely to be responsible for maintaining the overall
139 connectivity of the network. They are more likely to be essential genes or involved in critical
140 PPIs than non-hub nodes [44]. We identified 40 HUB nodes using manual curation based on
141 network centralities and connectivity, MCC, and MCODE algorithms[44–46]. Using betweenness
142 centrality and degree distribution, we manually curated 27 HUB nodes (Figure 3D-E). We
143 validated the HUBs using the MCODE and MCC clustering algorithms [45,46]. MCODE clustering
144 confirmed 26 of our 27 manually curated nodes as HUBs with scores $\geqslant 4$. The MCC clustering
145 algorithm confirmed 14 HUB nodes defined by manual curation and MCODE clustering and
146 suggested 13 additional HUB proteins (Figure 3B, Supplementary Dataset S8). Interestingly,
147 eight of the HUB proteins were reported to be essential for *L. crescens*[47], and 24 are known to be
148 essential in other bacteria[48].

149 **Inferring functions of CLas hypothetical proteins.** CLas contains 415 uncharacterized
150 proteins, including proteins annotated as hypothetical proteins, function unknown, or not in a
151 COG[4,49]. The CLas_HC network contained 1485 high-confidence interactions involving 160
152 uncharacterized proteins. The features of these proteins include: 15 have signal peptides that may

153 direct them to the cell membrane or outside the cell; 13 are secreted by a nonclassical pathway
154 that does not involve signal peptides; 27 have transmembrane domains that span the cell
155 membrane; and 107 have no assigned COG that indicates their function[4,36,50–52]. One hundred
156 forty-nine uncharacterized proteins interacted with at least one annotated protein, and 105
157 interacted with two or more proteins with known functions (Supplementary Dataset S3).

158 To infer the functions of those uncharacterized proteins based on their interacting partners, we
159 employed four guilt-by-association (GBA) methods: 1. Binary interactions and interologs, 2.
160 Operon associations, 3. Protein family associations, and 4. Meta-interactome analysis (Figure 4
161 illustrates each analysis method)[15,53–55].

162 *Inferring CLas protein functions from binary interactions.* Interologs are conserved interactions
163 between proteins whose homologs interact in other organisms [11]. As aforementioned, we
164 identified 635 interologs between 208 protein pairs in the CLas_whole network (Supplementary
165 Datasets S5 and S6). Among them, 34 were uncharacterized proteins. We have assigned
166 functions to four proteins based on interacting partners and similarities between proteins and
167 their 3D structures (Extended Data Figure S4). CLIBASIA_RS03480 was reannotated as
168 $FlgN_{Las}$, a flagellar switch chaperone, because it interacted with $FlgK_{Las}$ and $FlgL_{Las}$ proteins
169 involved in flagellar hook formation in the CLas network (Figure 4A, Extended Data Figure
170 S4A). The interactions between these proteins are well documented and are interologs found in
171 *S. meliloti* and *A. radiobacter* (Figure 4A)[56]. Similarly, we reannotated CLISASIA_RS03395 as
172 $FliK_{Las}$, a flagellar length regulator, because of its interactions with $FlgD_{Las}$, $FlhB_{Las}$, and $FliP_{Las}$
173 (Extended Data Figure S4B), three proteins involved in flagellar motor assembly, in the CLas
174 network[57–60]. Additionally, CLas hypothetical proteins CLIBASIA_RS03285 and
175 CLIBASIA_RS03885 were annotated as $TolA_{Las}$ and $YcgR_{Las}$ respectively (Extended Data
176 Figure S4C-D).

177 *Inter- and Intra- operon binary interaction topology gives functional association to CLas*
178 *uncharacterized proteins.* Next, we took advantage of the fact that bacterial genes of related
179 functions are transcribed together under a single promoter as operons[61]. We reasoned that
180 operons with known proteins interacting with the operons containing uncharacterized proteins
181 provide functional associations/clues for those groups of uncharacterized proteins. For this
182 purpose, we only considered inter- and intra-operon interactions where two or more proteins

183 from each operon interacted together for further analysis (Supplementary Dataset 9). We
184 examined how the PPIs of other organisms relate to the CLas Y2H network, specifically inter-
185 and intra-operon PPIs (Figure 4B and Extended Data Figure S5). We found that CLas had more
186 inter-operon PPIs than intra-operon interactions (Supplementary Datasets S9 and S10) compared
187 to interactions between homologous proteins. These inter-operon interactions provided evidence
188 of functional association of three CLas operons (638, 603, and 643), which consist of 21
189 uncharacterized proteins. Specifically, our interactome data demonstrated that CLas operon 638
190 has a functional association with flagellar assembly, stress response-related proteins, 50s
191 ribosomal proteins, cell division, and cell wall integrity proteins (Figure 4B). In addition, CLas
192 operon 603 has a functional association with translation, FeS cluster assembly, and succinate
193 dehydrogenase. In contrast, CLas operon 643 has a functional association with metabolism,
194 enzymes, and translation, in addition to FeS cluster assembly and succinate dehydrogenase
195 (Extended Data Figure S5).

196 *Protein family associations within the CLas Y2H network give clues to protein function.* We
197 evaluated PPIs between hypothetical proteins and CLas proteins within known protein families
198 or functions from the Kyoto Encyclopedia of Genes and Genomes (KEGG)[62]. Sixty-one CLas
199 proteins with unknown functions interacted with two or more proteins from the same protein
200 family or function in the CLas_HC Y2H network. These interactors were primarily involved in
201 metabolism and genetic information processing, as shown in examples of protein association
202 networks for CLIBASIA_RS04735 and CLIBASIA_RS04405 (Figure 4C). Operon associations
203 for eleven hypothetical proteins mirrored their KEGG associations, supporting the functional
204 assignment of eleven reannotated proteins (Supplementary Datasets S11 and S12; Extended Data
205 Tables S3 and S4).

206 *The CLas "meta-interactome" supports protein family association annotations and provides*
207 *evidence for additional hypothetical proteins.* As a final sweep of the Y2H data, we looked for
208 associations in a meta-interactome[15]. We generated a meta-interactome (mY2H) using
209 experimentally confirmed PPIs for *A. radiobacter, B. subtilis*, *C. jejuni*, *E. coli, H. pylori, L.*
210 *crescens*, *M. genitalium*, *M. loti*, *M. pneumoniae, S. cerevisiae, S. meliloti,* and *T. pallidum*. The
211 CLas mY2H has 12,780 edges between its 542 proteins (Figures 4D, Extended Data Figure S6).
212 Notably, most interactions (not including the CLas_whole Y2H PPIs) in the mY2H were PPIs in
213 *M. loti*, totaling 2296 edges. *M. loti* is more closely related to CLas than other organisms with

214 available Y2H interactome maps, such as *E. coli* and *H. pylori* [8,20,21,23]. We identified 416 CLas
215 proteins with orthologs among the 542 proteins in the mY2H, which contained 12,780 PPIs. Of
216 these PPIs, 635 PPI interologs between 208 protein pairs were conserved in the CLas_whole,
217 whereas 4037 were not (Supplementary Dataset S13). We used the orthologous PPI subnetworks
218 and the CLas protein associations from the mY2H to infer the functions of 26 uncharacterized
219 CLas proteins (Figures 4D, Extended Data Figure S6; Supplementary Dataset S12; Extended
220 Data Tables S3 and S4).

221 **Novel interactions identified for CLas proteins with known functions.** The CLas_whole
222 network identified 4245 interactions between 542 proteins (Figure 1B). Among the 371 CLas
223 proteins with known functions (Extended Data Tables S2 and S3), we identified 1654
224 interactions, whereas their homologs had 171 unique experimentally verified interactions in
225 previous studies [8,15–18,20–23,63]. This study identified 1483 novel PPIs that have not been
226 previously reported for proteins with known functions (Supplementary Dataset S14).

227 **Y2H PPIs related to Flagellar proteins.** Flagellar motility might play critical roles in CLas
228 infection of different organs of psyllids and movement in phloem tissues. Importantly, active
229 movement of CLas was observed in the phloem tissue against the flow of phloem sap[37,64]. We
230 paid close attention to flagella-related proteins. Our Y2H screening detected a total of 399
231 interactions among known flagellar proteins in our Y2H screening (Fig. 5; Supplementary
232 Dataset S15; Extended Data Tables S6, S7, and S8). In addition, nine interactions were
233 confirmed with pull-down assays (Fig. 2). Of those PPIs confirmed, two were putative secreted
234 proteins, CLIBASIA_RS05050[52] and CLIBASIA_RS05465[50], interacting with each other and
235 $FlgB_{Las}$, a flagellar basal-body protein[65]. Another secreted protein, CLIBASIA_RS03890, also
236 interacted with $FlgB_{Las}$[65]. These interactions imply that these proteins may play a role in flagellar
237 formation and functions, which could affect the pathogenicity or survival of CLas[50,66–68]. FlgN is
238 a known flagellar export chaperone of FlgK and FlgL, two hook-filament junction proteins[56]. We
239 also identified SecB, a chaperone protein dedicated to translocating proteins across the
240 cytoplasmic membrane, as an interactor of FlgK. We validated both interactions, $FlgK_{Las}$-$FlgN_{Las}$
241 and $FlgK_{Las}$-$SecB_{Las}$, consistent with the involvement of the Sec pathway in flagellar
242 synthesis[69,70]. Moreover, $SecB_{Las}$ interacted with CLIBASIA_RS0005, a protein with T-SNARE-
243 like domains. T-SNARE proteins mediate membrane fusion in eukaryotic cells. Pathogens can
244 exploit host SNARE proteins to enter host cells by displaying SNARE-like domains on their

surface membrane[71]. It remains to be determined whether CLIBASIA_RS0005 is involved in CLas entering cells or glands of psyllids[72].

Discussion

We have constructed the first and only large-scale protein-protein interaction map of CLas using a high-throughput Y2H approach. In total, we have identified 4245 PPIs among CLas proteins. We have employed a three-phase screening approach to improve the robustness of the Y2H. We estimated that our high-throughput Y2H data has a false positive rate of 3.1%, consistent with previously reported false positive rates of 0.5%[73], less than 5%[74], and 6.5%[75]. The pull-down assay supported the robustness of our Y2H.

Two hundred and eight binary PPIs, of the 4245 PPIs detected in this study, had been reported in previous studies[7,8,15–23,35,63,76]. On the other hand, 4037 novel interactions were identified in this study, expanding the PPI database. Two thousand five hundred eighty-three interactions involved 171 uncharacterized CLas proteins were identified, providing clues for their functions. For instance, we have assigned protein functions to CLIBASIA_RS03480 as FlgN, CLIBASIA_RS01260 as FliK, CLIBASIA_RS03285 as TolA, and CLIBASIA_RS03885 as YcgR. CLIBASIA_RS04860 and CLIBASIA_RS02370 might play a role in cell division since they interact with $FtsW_{Las}$ and $FtsQ_{Las}$, two essential components of the divisome complex[77]. These proteins interact with a HUB protein CLIBASIA_RS00450, CLIBASIA_RS05515, and RlpA (septal ring lytic transglycosylase, CLIBASIA_4130; $RlpA_{Las}$). RlpA is known to be involved in cell separation and rod shape of bacteria[78]. Thus, even though the functions of CLIBASIA_RS04960, CLIBASIA_RS02370, CLIBASIA_RS00450, and CLIBASIA_RS05515 are unknown, they are probably involved in cell division or cell wall formation, providing hints for further characterization. We have identified 37 uncharacterized proteins that interact with multiple proteins of an operon, and 61 uncharacterized proteins interacted with two or more proteins from the same family or function, providing strong indications regarding their roles associated with the known functions of the operons or protein families compared to single interactions. Among the 1662 interactions between proteins with known functions of CLas, only 171 have been observed in other systems, indicating that CLas proteins might have new functions to adapt to the reduced genome size. CLas, *T. pallidum*, and *M. pneumoniae* have a greater number of interactions per node in their PPI networks than free-living bacteria with larger

genomes, such as *E. coli*, *M. loti*, *H. pylori*, *C. jejuni*, and *B. subtilis*. An increase in node neighbors seems to be a common phenomenon for bacteria that have undergone reductive evolution[42].

We identified 40 putative HUB nodes in the network [45,79–81]. HUB proteins are suggested to be essential to the organism or involved in critical PPIs[22,38,79,80,82]. Eight of the HUB proteins were reported to be essential for *L. crescens*[47], and 24 are known to be essential in other bacteria[48]. Interestingly, multiple HUB proteins of CLas protect the bacteria from oxidative stress damage, including quinone oxidoreductase 1[83] and LysR-type transcriptional regulator[84]. Quinone oxidoreductase 1 acts as a cytoplasmic antioxidant, whereas LysR is a key circuit component in regulating microbial stress responses and is required for bacterial tolerance to H_2O_2 in vitro[84]. The protective mechanism of CLas is consistent with the model that HLB is a pathogen-triggered immune disease; CLas triggers systemic and chronic overproduction of reactive oxygen species, leading to phloem tissue cell death and HLB symptoms[85]. Thus, those proteins will protect CLas from the high ROS levels in the phloem tissues. Another HUB protein CtrA, is known to regulate bacterial cells, such as *Caulobacter crescentus*, to generate cells of different morphologies: with and without flagella[86]. Interestingly, CLas seems to encode most flagellar genes even though flagella have not been observed in CLas[37]. The extensive PPIs involving flagellar proteins suggest they are functional, consistent with the active movement of CLas against the flow of phloem sap [37,64]. CLas was also reported to be polymorphic in shape[37]. CtrA may be involved in the non-flagellated and polymorphic phenotypes of CLas cells in phloem tissues. Furthermore, ten of the 40 HUB genes are significantly up-or down-regulated in either citrus or ACP vector[87], suggesting they play crucial roles for CLas survival in citrus or psyllids.

Overall, we have generated the interactome map for CLas, which has provided insights regarding the biology and pathogenicity of CLas and the putative functions of uncharacterized proteins. This interactome will serve as a valuable resource and provide clues to further characterize the functions of unknown proteins. The PPIs identified have the potential to be used as targets for the development of novel antimicrobials to control HLB.

Methods

Yeast Two-hybrid vector construction. Full-length CLas ORFs were PCR amplified using genomic DNA extracted from CLas-positive citrus leaf tissues. The gel-purified amplicons were

305 fused with the activation (AD) and binding domain (BD) Y2H expression vectors (pGADT7 and
306 pGEO_BD, respectively) using infusion recombinase cloning (Clontech). We modified the Gal4
307 Matchmaker Gold Yeast Two-hybrid system (clonetech) pGBK_T7 (Clontech) expression vector
308 to harbor the pGADT7_AD vector's multiple cloning site (MCS) between RE sites NdeI and
309 BamHI (Extended Data Figure S1B) and was named pGEO_BD. This modification simplified
310 the cloning of all CLas ORFs into both vectors between RE sites EcoRI and XmaI using one
311 infusion primer set per gene to reduce costs and labor. These AD and BD infusion reactions (~20
312 µl per 50 µl reaction) were directly transformed into yeast strains Y187 (AD, prey clones;
313 MATa; G1::lacZ, M1::MEL1) and Y2H Gold (BD, bait clones; MATα; G1::HIS3, G2::ADE2,
314 M1::AUR1-C, M1::MEL1) following Yeastmaker Yeast Transformation protocol (Clontech).
315 We verified transformants with colony PCR and sequencing a random set of ~200 constructs.

316 **Autoactivation test.** Autoactivation of the reporter genes by individual ORFs was assessed by
317 mating the transformants with the opposite corresponding mating partner empty vector and
318 plating on selective media DDO/X/AbA (-Leu, -Trp, + XαGal, +Aureobasidin A). Clones that
319 autonomously activated reporter genes were removed from the 96-well plates and high
320 throughput screening.

321 **Yeast Two-hybrid three-phase screening.** A three-phase 96-well mating scheme was adapted
322 from a matrix approach[32]. Briefly, all transformants were cultured individually in 96-well plates
323 in 1 ml of the appropriate minimal liquid media (AD: -Leu; BD: -Trp) at 30°C until saturated
324 (~36-48 hours). For the first mating phase (three phases in total), all individual 1 ml AD cultures
325 were pooled together and centrifuged at 700 g for 5 min. The pellet was resuspended in 25 ml
326 SD/-Leu liquid media with 25% glycerol. Aliquots (1 ml) of the pool were stored at -80°C. The
327 BD cultures were left in a 96-well format for the phase 1 mating.

328 **Mating procedure. *Phase 1.*** Each AD pool was mated to individual pGEO_BD clones in a 96-
329 well format. The matings were spotted on YPDA agar plates by spotting 3 µl of the AD pool
330 aliquot and 3 µl of the individual BD clone on top of one another and incubated at 30°C for ~ 48
331 hrs, or until the colonies were ~ 1 mm in diameter. The 1 mm colonies were transferred using a
332 pin replicator to 96-well plates with DDO (-Leu, -Trp) liquid medium to select diploids
333 harboring AD and BD plasmids and incubated at 30°C and 210 rpm on a rotary shaker. This step
334 reduces the background on the selection plates. After 48 hrs, five µl of the mating cultures were

335 plated on DDO (-Leu, -Trp) agar plates as a mating control, and selective media to determine
336 interaction and interaction intensity: D/X/A (-Leu, -Trp, + XαGal, +Aureobasidin A), Q/X (-Leu,
337 -Trp, -His, -Ade + XαGal), and Q/X/A (-Leu, -Trp, -His, -Ade + XαGal, +Aureobasidin A). All
338 subsequent matings and screenings were carried out in the same manner. ***Phase 2.*** Positive BD
339 clones from the phase 1 mating were pooled using the previously described AD pooling method.
340 These BD pools (containing all positive BD interactors from phase 1) were mated back to the
341 AD plate that comprised the pool of phase 1. This is to determine which of the AD clones within
342 the pool were the interacting partners to the positive BD interactors from phase 1 (Figure 1A**)**.
343 ***Phase 3.*** The final phase determined the interacting partners from the previous two screenings
344 and allowed for a pairwise rescreening of all interacting constructs. All positive AD and BD
345 yeast constructs interacting in the first two phase screenings were organized into a row (BD) and
346 column (AD) format in 96-well plates. Each row of a 96-well plate is a single BD construct (For
347 example, row A: BD construct #1, row B: BD construct #2, row C: BD construct #3… to row H:
348 BD construct #8) and each column is a single AD construct (For example column 1: AD
349 construct #1, column 2: AD construct #2, column 3: AD construct #3… to column 12: AD
350 construct #12) which were mated pairwise. The row and column format allowed all phase one
351 and two proteins to interact to determine the interacting partners and the interaction specificity.
352 This method helped determine what interactions are more likely, or accurate since interactions
353 must be repeatable pairwise and allowed us to weed out sticky interactors.

354 **Analysis of the CLas Y2H network topology.** We visualized, analyzed, and utilized the
355 network developed in this study with Cytoscape network software (Shannon et al., 2003).
356 Network topologies, such as betweenness and closeness centrality, degree, and clustering
357 coefficient, were determined using the Network Analyzer in Cytoscape (Assenov et al., 2008).
358 We used this information to select HUB nodes in the network for further analysis and understand
359 general CLas interactome network organization found in the Y2H screening. To validate the
360 CLas_whole network topology, NetworkRandomizer version 3 was used to compare the
361 CLas_whole network to a randomly computed network. We compared the difference between
362 the real network (CLas_whole) and its most similar random network for each centrality[88].

363 Hub nodes were determined using manual curation, MCODE clustering, and MCC
364 algorithm[44,89,90].

365 **Scoring interactions and assigning interaction confidence values.** PPIs were scored on a scale
366 from one to three for each selection media. These colony scores were used with PPI interologs,
367 PPIs within the same operon, and bait out-degree and prey in-degree to create an additive score
368 for the logistic regression formula to assign interaction confidence scores. The logistic regression
369 training set of 100 interologs was used as true positives and 100 PPIs with the lowest combined
370 Y2H score and highest average shortest path link value with randomized bait and prey node
371 degree values, as true negatives. We calculated the interaction scoring four times using different
372 variables for each regression. The variables were: the number of times as a bait, number of times
373 as a prey, interolog score alone, and interolog score combined with Y2H repeatability and
374 interaction intensity. We averaged the values from each regression to obtain the final interaction
375 confidence score [16].

376 $$\textit{Interaction Score} = \frac{1}{1+e^{-(-178.67-(-2.25484)*bc-0.4624*pc+506.1149*cs)}};$$

377 *bc: count of occurrence as a bait node; pc: count of occurrence of prey node; cs: colony score*

378 **Conserved protein-protein interactions (interologs).** CLas homologs in *A. radiobacter, B.*
379 *subtilis*, *C. jejuni*, *E. coli, H. pylori, L. crescens*, *M. genitalium*, *M. loti*, *M. pneumoniae, S.*
380 *cerevisiae, S. meliloti, T. pallidum,* and iCOGs were collected using IMG/MER and NCBI
381 databases [16,21,91,92]. Only protein sequences with an identity of >30% were considered for
382 analysis. All available experimentally determined (i.e., Y2H, AP/MS, and CO-IP) ortholog PPIs
383 and iCOG PPIs were collected from the STRING database for these homologs[16]. The known and
384 predicted interactions between CLas proteins were also included in the data collected from
385 STRING[35].

386 **Validating CLas interactions *in vivo* by a pairwise Y2H screening.** We randomly chose 163
387 ORF constructs (15.9% of the total CLas ORFs and 30% of the nodes in the CLas_whole
388 network) to use in a pairwise Y2H screening. The interactions from this screening were
389 compared for overlap between the three datasets: the pairwise screening, the three-phase Y2H
390 PPI screening, and the known and predicted interactions between these proteins available from
391 the STRING database. The rates of false positives, false negatives, specificity, and sensitivity
392 within the three-phase screening were determined using the known interactions and pairwise
393 screening[93].

394 **Confirming CLas interactions using pull-down assay.** Interactions were validated using
395 MBP/GST pull-down assay. The pGEX-4T-1 (GST) (GE Healthcare) and pMAL-c5x (MBP)
396 (NEB) vectors were used to construct the *E. coli* expression vectors for GST-Glutathione and/or
397 MBP-Amylose pull-down assay between multiple CLas proteins. The GST/MBP expression
398 vectors were constructed by amplifying the ORFs from the CLas yeast expression vectors and
399 inserted between RE sites: BamHI and SalI in pGEX vector and XmnI and EcoRI in pMAL
400 vector using infusion cloning (Clontech). These newly generated vector constructs were
401 transformed into *E. coli* Rosetta (DE3) electrocompetent cells, transformants were selected by
402 plating on LB agar plates containing ampicillin (100 µg/ml) and chloramphenicol (30 µg/ml); all
403 subsequent steps used these antibiotics at these concentrations. The transformants were cultured
404 overnight in 3 ml liquid LB. The next day, the culture was diluted 1:100 in 25 ml LB and grown
405 until the culture reached an OD_{600} 0.2-0.3. The culture was then induced with IPTG (1 µg/ml)
406 overnight at 16°C.

407 After induction, the resulting cell pellet was lysed using 5 µg/ml of pellet with B-PER™
408 Bacterial Protein Extraction Reagent (Thermo-Fisher) and incubated at room temperature for 20
409 minutes while rocking. The lysates were cleared by centrifugation at 4°C for 20 minutes at
410 16,000 g. Supernatants were collected in a fresh tube and total protein concentration was
411 measured using Bradford assay. The protein expression and solubility were evaluated by both
412 Coomassie stain and western blot (WB) of the GST and MBP fusion proteins using anti-GST
413 (abcam) and anti-MBP (NEB) monoclonal antibodies before proceeding. The GST-fusion
414 protein and empty-GST supernatants were mixed with the MBP-fusion protein and incubated
415 with glutathione or amylose agarose beads for 3-4 hours at 4°C with rotating. The glutathione or
416 amylose agarose was then washed 5-10 times to remove unbound proteins before boiling and
417 analysis by SDS-PAGE WB using anti-MBP (NEB) and anti-GST (abcam) monoclonal
418 antibodies. Protein-protein interactions that were further confirmed by pull-down assays were
419 shown in T Extended Data Table S9.

420 **Data availability**

421 The data related to Y2H assays were included in the datasets or supplementary tables.

422

423 **REFERENCES**

1. Yuan, X. *et al.* Region-wide comprehensive implementation of roguing infected trees, tree replacement, and insecticide applications successfully controls citrus huanglongbing. *Phytopathology* **111**, (2021).

2. Singerman, A. & Rogers, M. E. The Economic Challenges of Dealing with Citrus Greening: The Case of Florida. *J Integr Pest Manag* **11**, (2020).

3. Wang, N. *et al.* The Candidatus Liberibacter-Host Interface: Insights into Pathogenesis Mechanisms and Disease Control. *Annual Review of Phytopathology* vol. 55 Preprint at https://doi.org/10.1146/annurev-phyto-080516-035513 (2017).

4. Duan, Y. *et al.* Complete genome sequence of citrus huanglongbing bacterium, '*Candidatus* Liberibacter asiaticus' obtained through metagenomics. *Molecular Plant-Microbe Interactions* **22**, (2009).

5. Merfa, M. V. *et al.* Progress and Obstacles in Culturing '*Candidatus* Liberibacter asiaticus', the Bacterium Associated with Huanglongbing. *Phytopathology* vol. 109 Preprint at https://doi.org/10.1094/PHYTO-02-19-0051-RVW (2019).

6. Kühner, S. *et al.* Proteome organization in a genome-reduced bacterium. *Science (1979)* **326**, (2009).

7. Ito, T. *et al.* A comprehensive two-hybrid analysis to explore the yeast protein interactome. *Proc Natl Acad Sci U S A* **98**, (2001).

8. Rain, J. C. *et al.* The protein-protein interaction map of *Helicobacter pylori*. *Nature* **409**, (2001).

9. Cossar, P. J., Lewis, P. J. & McCluskey, A. Protein-protein interactions as antibiotic targets: A medicinal chemistry perspective. *Medicinal Research Reviews* vol. 40 Preprint at https://doi.org/10.1002/med.21519 (2020).

10. Giot, L. *et al.* A Protein Interaction Map of Drosophila melanogaster. *Science (1979)* **302**, (2003).

11. Vidal, M. Protein interaction mapping in C. elegans Using proteins involved in vulval development. *Science (1979)* **287**, (2000).

12. Li, S. *et al.* A Map of the Interactome Network of the Metazoan C. elegans. *Science (1979)* **303**, (2004).

13. Brandão, M. M., Dantas, L. L. & Silva-Filho, M. C. AtPIN: Arabidopsis thaliana protein interaction network. *BMC Bioinformatics* **10**, (2009).

455 14. Braun, P. *et al.* Evidence for Network Evolution in an Arabidopsis Interactome
456 Map. *Science (1979)* **333**, (2011).

457 15. Wuchty, S. *et al.* The Protein Interactome of *Streptococcus pneumoniae* and
458 Bacterial Meta-interactomes Improve Function Predictions. *mSystems* **2**, (2017).

459 16. Titz, B. *et al.* The binary protein interactome of *Treponema pallidum* - The syphilis
460 spirochete. *PLoS One* **3**, (2008).

461 17. Parrish, J. R. *et al.* A proteome-wide protein interaction map for *Campylobacter*
462 *jejuni*. *Genome Biol* **8**, (2007).

463 18. Sato, S. *et al.* A large-scale protein-protein interaction analysis in *Synechocystis* sp.
464 PCC6803. *DNA Research* **14**, (2007).

465 19. Wang, Y. *et al.* Global protein-protein interaction network in the human pathogen
466 *Mycobacterium tuberculosis* H37Rv. *J Proteome Res* **9**, (2010).

467 20. Shimoda, Y. *et al.* A large scale analysis of protein-protein interactions in the
468 nitrogen-fixing bacterium *Mesorhizobium loti*. *DNA Research* **15**, (2008).

469 21. Rajagopala, S. V. *et al.* The binary protein-protein interaction landscape of
470 *Escherichia coli*. *Nat Biotechnol* **32**, (2014).

471 22. Marchadier, E. *et al.* An expanded protein-protein interaction network in *Bacillus*
472 *subtilis* reveals a group of hubs: Exploration by an integrative approach. *Proteomics*
473 **11**, (2011).

474 23. Hauser, R. *et al.* A second-generation protein-protein interaction network of
475 *Helicobacter pylori*. *Molecular and Cellular Proteomics* **13**, (2014).

476 24. Meseguer, M. A. *et al. Mycoplasma pneumoniae*: A reduced-genome intracellular
477 bacterial pathogen. *Infection, Genetics and Evolution* **3**, (2003).

478 25. Schwikowski, B., Uetz, P. & Fields, S. A network of protein-protein interactions in
479 yeast. *Nat Biotechnol* **18**, (2000).

480 26. Galperin, M. Y. & Koonin, E. v. SURVEY AND SUMMARY 'Conserved
481 hypothetical' proteins: prioritization of targets for experimental study.
482 doi:10.1093/nar/gkh885.

27. Barabási, A. L. & Oltvai, Z. N. Network biology: Understanding the cell's functional organization. *Nature Reviews Genetics* vol. 5 Preprint at https://doi.org/10.1038/nrg1272 (2004).

28. Typas, A. & Sourjik, V. Bacterial protein networks: Properties and functions. *Nature Reviews Microbiology* vol. 13 Preprint at https://doi.org/10.1038/nrmicro3508 (2015).

29. Yook, S. H., Oltvai, Z. N. & Barabási, A. L. Functional and topological characterization of protein interaction networks. *Proteomics* **4**, (2004).

30. Cao, F. Y. *et al.* A host-pathogen interactome uncovers phytopathogenic strategies to manipulate plant ABA responses. (2019) doi:10.1111/tpj.14425.

31. Asensio, N. C., Giner, E. M., Sánchez De Groot, N. & Burgas, M. T. ARTICLE Centrality in the host-pathogen interactome is associated with pathogen fitness during infection. *Nat Commun* (2017) doi:10.1038/ncomms14092.

32. Zhong, J., Zhang, H., Stanyon, C. A., Tromp, G. & Finley, R. L. A strategy for constructing large protein interaction maps using the yeast two-hybrid system: Regulated expression arrays and two-phase mating. *Genome Res* **13**, (2003).

33. Goll, J. & Uetz, P. The elusive yeast interactome. *Genome Biology* vol. 7 Preprint at https://doi.org/10.1186/gb-2006-7-6-223 (2006).

34. Rajagopala, S. V. Mapping the protein–protein interactome networks using yeast two-hybrid screens. in *Advances in Experimental Medicine and Biology* vol. 883 (2015).

35. Szklarczyk, D. *et al.* The STRING database in 2021: Customizable protein-protein networks, and functional characterization of user-uploaded gene/measurement sets. *Nucleic Acids Res* **49**, (2021).

36. Galperin, M. Y. *et al.* COG database update: Focus on microbial diversity, model organisms, and widespread pathogens. *Nucleic Acids Res* **49**, (2021).

37. Andrade, M. O. *et al.* The flagella of '*Candidatus* Liberibacter asiaticus' and its movement in planta. *Mol Plant Pathol* **21**, (2020).

38. Zotenko, E., Mestre, J., O'Leary, D. P. & Przytycka, T. M. Why do hubs in the yeast protein interaction network tend to be essential: Reexamining the connection between the network topology and essentiality. *PLoS Comput Biol* **4**, (2008).

514 39. Hart, G. T., Lee, I. & Marcotte, E. R. A high-accuracy consensus map of yeast
515 protein complexes reveals modular nature of gene essentiality. *BMC Bioinformatics*
516 **8**, (2007).

517 40. Shannon, P. *et al.* Cytoscape: A software Environment for integrated models of
518 biomolecular interaction networks. *Genome Res* **13**, (2003).

519 41. Assenov, Y., Ramírez, F., Schelhorn, S. E. S. E., Lengauer, T. & Albrecht, M.
520 Computing topological parameters of biological networks. *Bioinformatics* **24**,
521 (2008).

522 42. Kelkar, Y. D. & Ochman, H. Genome reduction promotes increase in protein
523 functional complexity in bacteria. *Genetics* **193**, (2013).

524 43. Kuo, C. H., Moran, N. A. & Ochman, H. The consequences of genetic drift for
525 bacterial genome complexity. *Genome Res* **19**, (2009).

526 44. Jeong, H., Mason, S. P., Barabási, A. L. & Oltvai, Z. N. Lethality and centrality in
527 protein networks. *Nature* **411**, (2001).

528 45. Chin, C. H. *et al.* cytoHubba: Identifying hub objects and sub-networks from
529 complex interactome. *BMC Syst Biol* **8**, (2014).

530 46. Doyle, J. R. MCC-multiple correlation clustering. *Int J Man Mach Stud* **37**, (1992).

531 47. Lai, K. K., Davis-Richardson, A. G., Dias, R. & Triplett, E. W. Identification of the
532 genes required for the culture of *Liberibacter crescens*, the closest cultured relative
533 of the Liberibacter plant pathogens. *Front Microbiol* **7**, (2016).

534 48. Zhang, R., Ou, H. Y. & Zhang, C. T. DEG: A database of essential genes. *Nucleic*
535 *Acids Res* **32**, (2004).

536 49. Blake, J. A. *et al.* Gene ontology consortium: Going forward. *Nucleic Acids Res* **43**,
537 (2015).

538 50. Du, P. *et al.* "*Candidatus* Liberibacter asiaticus" Secretes Nonclassically Secreted
539 Proteins That Suppress Host Hypersensitive Cell Death and Induce Expression of
540 Plant Pathogenesis-Related Proteins. *Appl Environ Microbiol* **87**, (2021).

541 51. Beckwith, J. The Sec-dependent pathway. *Res Microbiol* **164**, (2013).

542 52. Prasad, S., Xu, J., Zhang, Y. & Wang, N. SEC-translocon dependent
543 extracytoplasmic proteins of *Candidatus* Liberibacter asiaticus. *Front Microbiol* **7**,
544 (2016).

545 53. Nguyen, P. V., Srihari, S. & Leong, H. W. Identifying conserved protein complexes
546 between species by constructing interolog networks. *BMC Bioinformatics* **14**,
547 (2013).

548 54. Oliver, S. Guilt-by-association goes global. *Nature* vol. 403 Preprint at
549 https://doi.org/10.1038/35001165 (2000).

550 55. Moreno-Hagelsieb, G. The power of operon rearrangements for predicting
551 functional associations. *Computational and Structural Biotechnology Journal* vol.
552 13 Preprint at https://doi.org/10.1016/j.csbj.2015.06.002 (2015).

553 56. Aldridge, P., Karlinsey, J. & Hughes, K. T. The type III secretion chaperone FlgN
554 regulates flagellar assembly via a negative feedback loop containing its chaperone
555 substrates FlgK and FlgL. *Mol Microbiol* **49**, (2003).

556 57. Eggenhofer, E., Rachel, R., Haslbeck, M. & Scharf, B. MotD of *Sinorhizobium*
557 *meliloti* and related α-proteobacteria is the flagellar-hook-length regulator and
558 therefore reassigned as FliK. *J Bacteriol* **188**, (2006).

559 58. Moriya, N., Minamino, T., Imada, K. & Namba, K. Genetic analysis of the bacterial
560 hook-capping protein FlgD responsible for hook assembly. *Microbiology (N Y)* **157**,
561 (2011).

562 59. Hirano, T., Yamaguchi, S., Oosawa, K. & Aizawa, S. I. Roles of FliK and FlhB in
563 determination of flagellar hook length in *Salmonella typhimurium*. *J Bacteriol* **176**,
564 (1994).

565 60. Aizawa, S. I. Bacterial flagella and type III secretion systems. *FEMS Microbiology*
566 *Letters* vol. 202 Preprint at https://doi.org/10.1016/S0378-1097(01)00301-9 (2001).

567 61. Osbourn, A. E. & Field, B. Operons. *Cellular and Molecular Life Sciences* vol. 66
568 Preprint at https://doi.org/10.1007/s00018-009-0114-3 (2009).

569 62. Kanehisa, M. & Goto, S. KEGG: Kyoto Encyclopedia of Genes and Genomes.
570 *Nucleic Acids Research* vol. 28 Preprint at https://doi.org/10.1093/nar/28.1.27
571 (2000).

572 63. Uetz, P. *et al.* A comprehensive analysis of protein-protein interactions in
573 *Saccharomyces cerevisiae*. *Nature* **403**, (2000).

574 64. Pandey, S. S., Hendrich, C., Andrade, M. O. & Wang, N. *Candidatus* Liberibacter:
575 From Movement, Host Responses, to Symptom Development of Citrus
576 Huanglongbing. *Phytopathology* vol. 112 Preprint at
577 https://doi.org/10.1094/PHYTO-08-21-0354-FI (2022).

578 65. Tan, J. *et al.* Structural basis of assembly and torque transmission of the bacterial
579 flagellar motor. *Cell* **184**, (2021).

580 66. Young, G. M., Schmiel, D. H. & Miller, V. L. A new pathway for the secretion of
581 virulence factors by bacteria: The flagellar export apparatus functions as a protein-
582 secretion system. *Proc Natl Acad Sci U S A* **96**, (1999).

583 67. Konkel, M. E. *et al.* Secretion of virulence proteins from *Campylobacter jejuni* is
584 dependent on a functional flagellar export apparatus. *J Bacteriol* **186**, (2004).

585 68. Costa, T. R. D. *et al.* Secretion systems in Gram-negative bacteria: Structural and
586 mechanistic insights. *Nature Reviews Microbiology* 13, 343–359 (2015).

587 69. Mobley HLT, Mendz GL, Hazell SL, editors. Helicobacter pylori: Physiology and
588 Genetics. Washington (DC): ASM Press (2001).

589 70. Tsirigotaki, A., De Geyter, J., Šoštarić, N., Economou, A. & Karamanou, S. Protein
590 export through the bacterial Sec pathway. *Nature Reviews Microbiology* vol. 15
591 Preprint at https://doi.org/10.1038/nrmicro.2016.161 (2017).

592 71. Wesolowski, J. & Paumet, F. SNARE motif: A common motif used by pathogens
593 to manipulate membrane fusion. *Virulence* **1**, (2010).

594 72. Ghanim, M., Fattah-Hosseini, S., Levy, A. & Cilia, M. Morphological
595 abnormalities and cell death in the Asian citrus psyllid (*Diaphorina citri*) midgut
596 associated with Candidatus Liberibacter asiaticus. *Sci Rep* **6**, (2016).

597 73. Venkatesan, K. *et al.* An empirical framework for binary interactome mapping. *Nat*
598 *Methods* **6**, (2009).

599 74. Braun, P. *et al.* An experimentally derived confidence score for binary protein-
600 protein interactions. *Nat Methods* **6**, (2009).

601 75. Chen, Y. C., Rajagopala, S. V., Stellberger, T. & Uetz, P. Exhaustive benchmarking
602 of the yeast two-hybrid system. *Nature Methods* vol. 7 Preprint at
603 https://doi.org/10.1038/nmeth0910-667 (2010).

604 76. Arifuzzaman, M. *et al.* Large-scale identification of protein-protein interaction of
605 Escherichia coli K-12. *Genome Res* **16**, (2006).

606 77. Errington, J. & Wu, L. J. Cell cycle machinery in Bacillus subtilis. *Subcell Biochem*
607 **84**, (2017).

608 78. Jorgenson, M. A., Chen, Y., Yahashiri, A., Popham, D. L. & Weiss, D. S. The
609 bacterial septal ring protein RlpA is a lytic transglycosylase that contributes to rod
610 shape and daughter cell separation in *Pseudomonas aeruginosa*. *Mol Microbiol* **93**,
611 (2014).

612 79. Batada, N. N., Hurst, L. D. & Tyers, M. Evolutionary and physiological importance
613 of hub proteins. *PLoS Comput Biol* **2**, (2006).

614 80. He, X. & Zhang, J. Why do hubs tend to be essential in protein networks? *PLoS*
615 *Genet* **2**, (2006).

616 81. Seo, C. H., Kim, J. R., Kim, M. S. & Cho, K. H. Hub genes with positive feedbacks
617 function as master switches in developmental gene regulatory networks.
618 *Bioinformatics* **25**, (2009).

619 82. Gollapalli, P., G, T. S., H, M., Shetty, P. & N, S. K. Network topology analysis of
620 essential genes interactome of Helicobacter pylori to explore novel therapeutic
621 targets. *Microb Pathog* **158**, (2021).

622 83. Qiu, D. *et al.* NAD(P)H: quinone oxidoreductase 1 attenuates oxidative stress and
623 apoptosis by regulating Sirt1 in diabetic nephropathy. *J Transl Med* **20**, (2022).

624 84. Reen, F. J., Haynes, J. M., Mooij, M. J. & O'Gara, F. A Non-Classical LysR-Type
625 Transcriptional Regulator PA2206 Is Required for an Effective Oxidative Stress
626 Response in *Pseudomonas aeruginosa*. *PLoS One* **8**, (2013).

627 85. Ma, W. *et al.* Citrus Huanglongbing is a pathogen-triggered immune disease that
628 can be mitigated with antioxidants and gibberellin. *Nat Commun* **13**, (2022).

629 86. Siam, R. & Marczynski, G. T. Cell cycle regulator phosphorylation stimulates two
630 distinct modes of binding at a chromosome replication origin. *EMBO Journal* **19**,
631 (2000).

87. de Francesco, A. *et al.* Transcriptome Profiling of '*Candidatus* Liberibacter asiaticus' in Citrus and Psyllids. *Phytopathology* **112**, (2022).

88. Tosadori, G., Bestvina, I., Spoto, F., Laudanna, C. & Scardoni, G. Creating, generating and comparing random network models with NetworkRandomizer. *F1000Res* **5**, (2017).

89. Morris, J. H. *et al.* ClusterMaker: A multi-algorithm clustering plugin for Cytoscape. *BMC Bioinformatics* **12**, (2011).

90. Hogue, C. W. & Groll, M. Mcode. *BMC Bioinformatics* **29**, (2001).

91. Johnson, M. *et al.* NCBI BLAST: a better web interface. *Nucleic Acids Res* **36**, (2008).

92. Markowitz, V. M. *et al.* IMG ER: A system for microbial genome annotation expert review and curation. *Bioinformatics* **25**, (2009).

93. YERUSHALMY, J. Statistical problems in assessing methods of medical diagnosis, with special reference to X-ray techniques. *Public health reports* **62**, (1947).

Acknowledgements

We thank Wang lab members for constructive suggestions and insightful discussions. This project was supported by funding from Florida Citrus Initiative Program, Citrus Research and Development Foundation, U.S. Department of Agriculture National Institute of Food and Agriculture grants 2022-70029-38471, 2021-67013-34588, 2018-70016-27412 and 2016-70016-24833, FDACS Specialty Crop Block Grant Program, and Hatch project [FLA-CRC-005979] (N. Wang).

Author Contributions

N.W. and E.W.C. conceptualized and designed the experiments. E.W.C. and O.G.P. designed the pGEO vector and oligonucleotides. E.W.C. performed the experiments. E.W.C. and N.W. wrote the manuscript with input from all co-authors.

Competing interests. All other authors declare no competing financial interests.

Correspondence and requests for materials should be addressed to N. Wang.

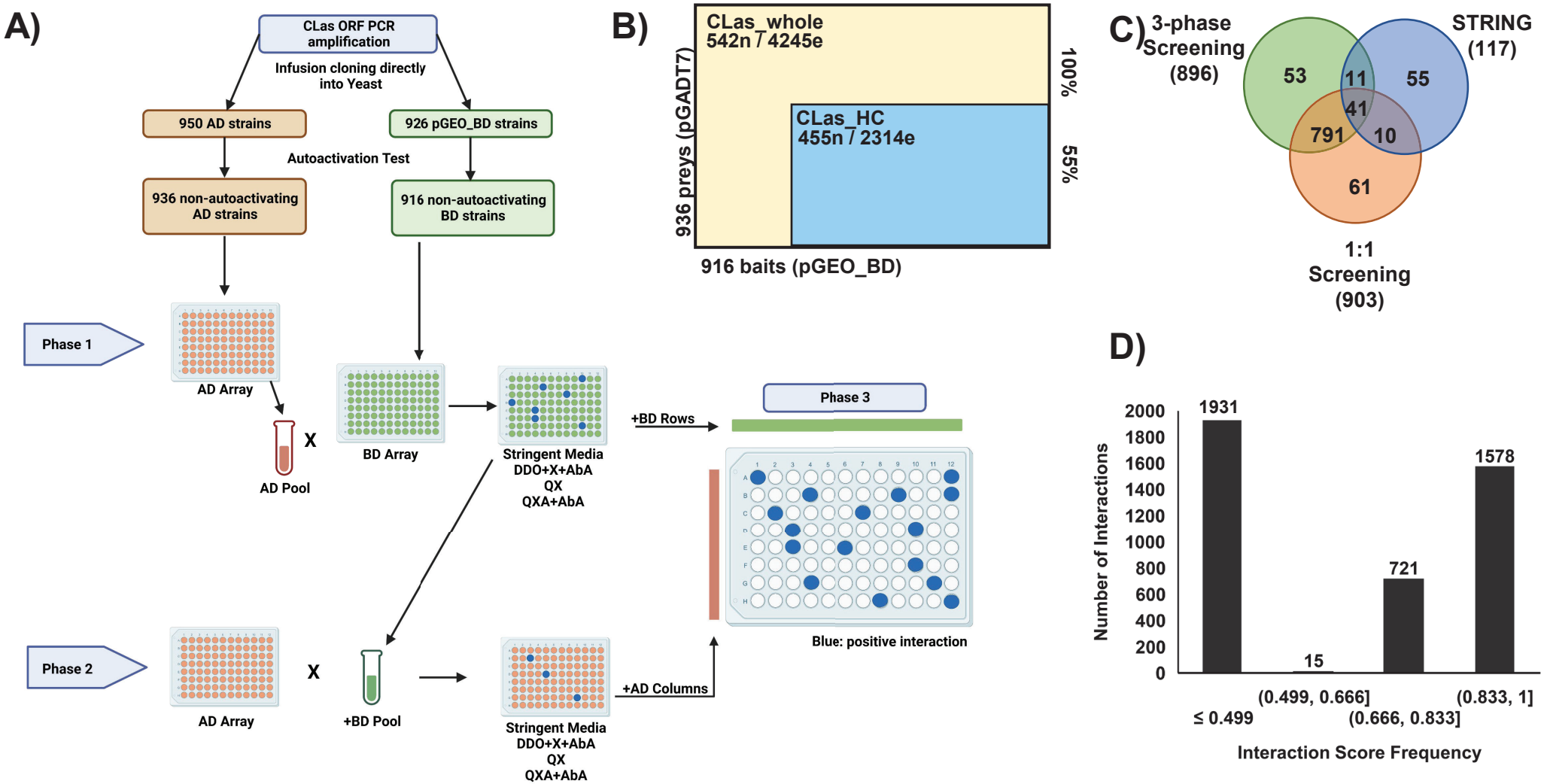

Figure 1. The CLas Y2H interactome screening, validation, and confidence scores. A. The three-phase 96-well plate screening pipeline for constructing the CLas_whole network. Phase one and two systematically screened pools and individual yeast constructs to identify potential interacting protein partners. All interacting partners were identified in the third phase in a pairwise screening; phase 1 and 2 interacting proteins were screened pairwise against all other phase 1 and 2 interacting proteins to produce the binary data. **B.** CLas Y2H three-phase screening results. n: node; e: edge; 100% indicates: CLas_whole network; 55% indicates: CLas_HC network portion of the CLas_whole network **C.** Venn diagram showing the overlap of interactions detected in the three-phase screening, an independent pairwise screening, and predicted interactions for 163 CLas proteins; predicted interactions were downloaded from the String consortium. **D.** Interaction confidence score frequency across the CLas_whole network. Interactions with a confidence score ≥0.5 are considered high confidence; denoted as the CLas_HC network.

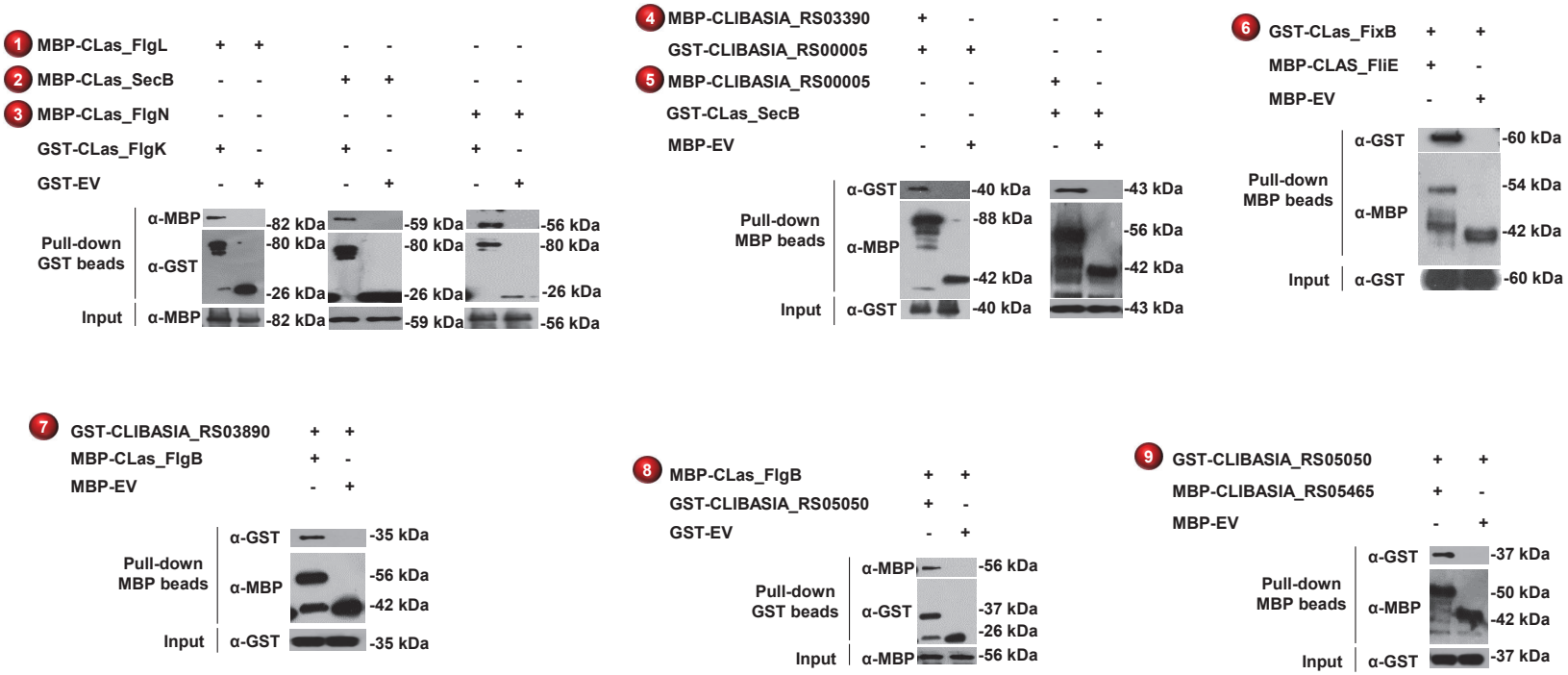

Figure 2. Confirmation of the PPIs identified in Y2H using pull-down assays. Both GST and MBP pull-down assays were conducted, dependent on protein pairs. Interactions confirmed *in vitro* are numbered for illustration in Fig. 5.

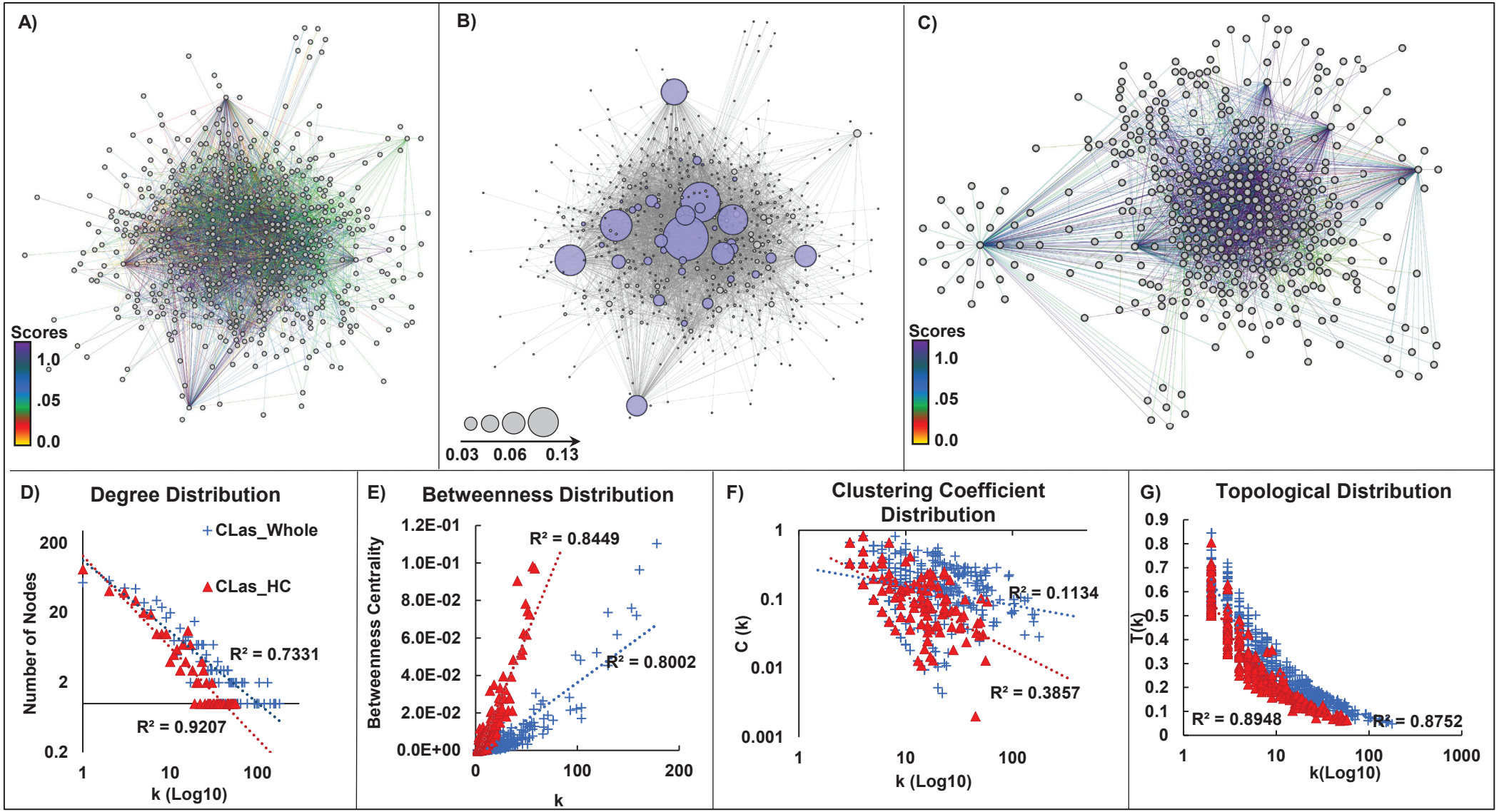

Figure 3. The CLas Y2H network topology. A-C. Graphic representation. n: node indicating a protein in the network; e: edge indicating the connection between the interacting proteins. **A.** CLas_whole network (542n,4245e). **B.** HUB nodes in the CLas_whole network are colored blue; node size is proportional to its betweenness centrality value. **C.** CLas_HC network; PPI confidence scores ≥0.5. **D-G.** Network topology of the CLas_whole and CLas_HC networks. **D.** Degree distribution. **E.** Betweenness centrality distribution. **F.** Clustering coefficient distribution. **G.** Topological coefficient distribution.

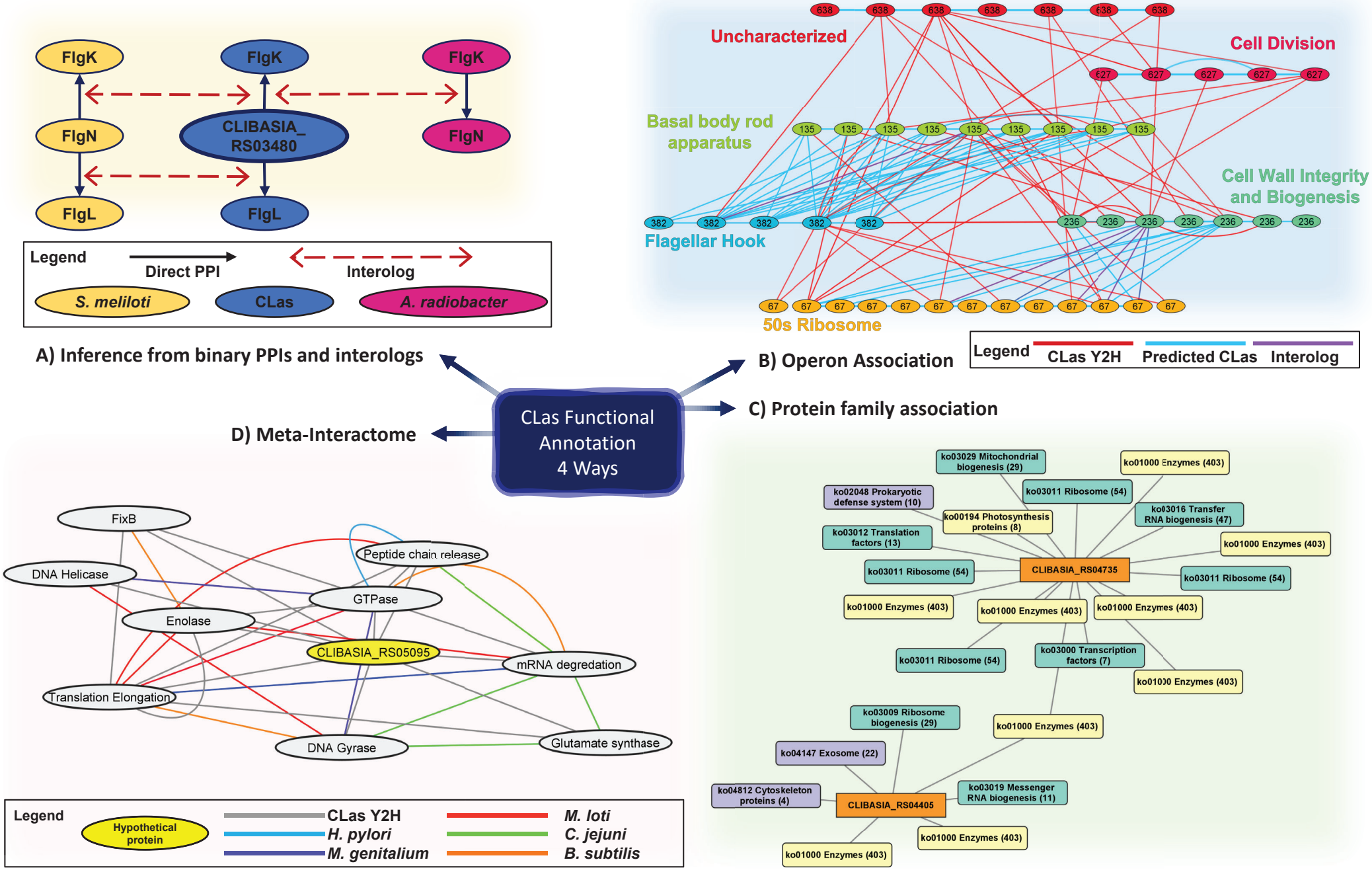

Figure 4. Four approaches were used to infer CLas hypothetical protein functional annotations. A. Inter-operon interactions highlight associations between motility related genes, respiration, membrane integrity, ribosomal proteins, and uncharacterized genes and operons. Operon associations, network and properties are in table S9. **B.** Hypothetical protein annotations were implied by interologs and binary interactions. These validity of the interactions were confirmed by *in vitro* assays and tertiary protein structure homology. **C.** Guilt by association was used for CLas proteins interacting with ≥2 proteins in the same protein family or KEGG pathway. CLIBASIA_RS04405 has a functional association with enzymatic proteins, ribosome and RNA biogenesis, and exosome, cytoskeleton proteins. The binary interactions between CLIBASIA_RS04735 and ribosome, transcription/translation proteins implies a functional association with cell response and growth. **D.** The sub network meta-interactome ($mY2H_{5095}$) for CLIBASIA_RS05095 whose protein function was inferred by its ortholog associations as having a putative association with genetic information processing.

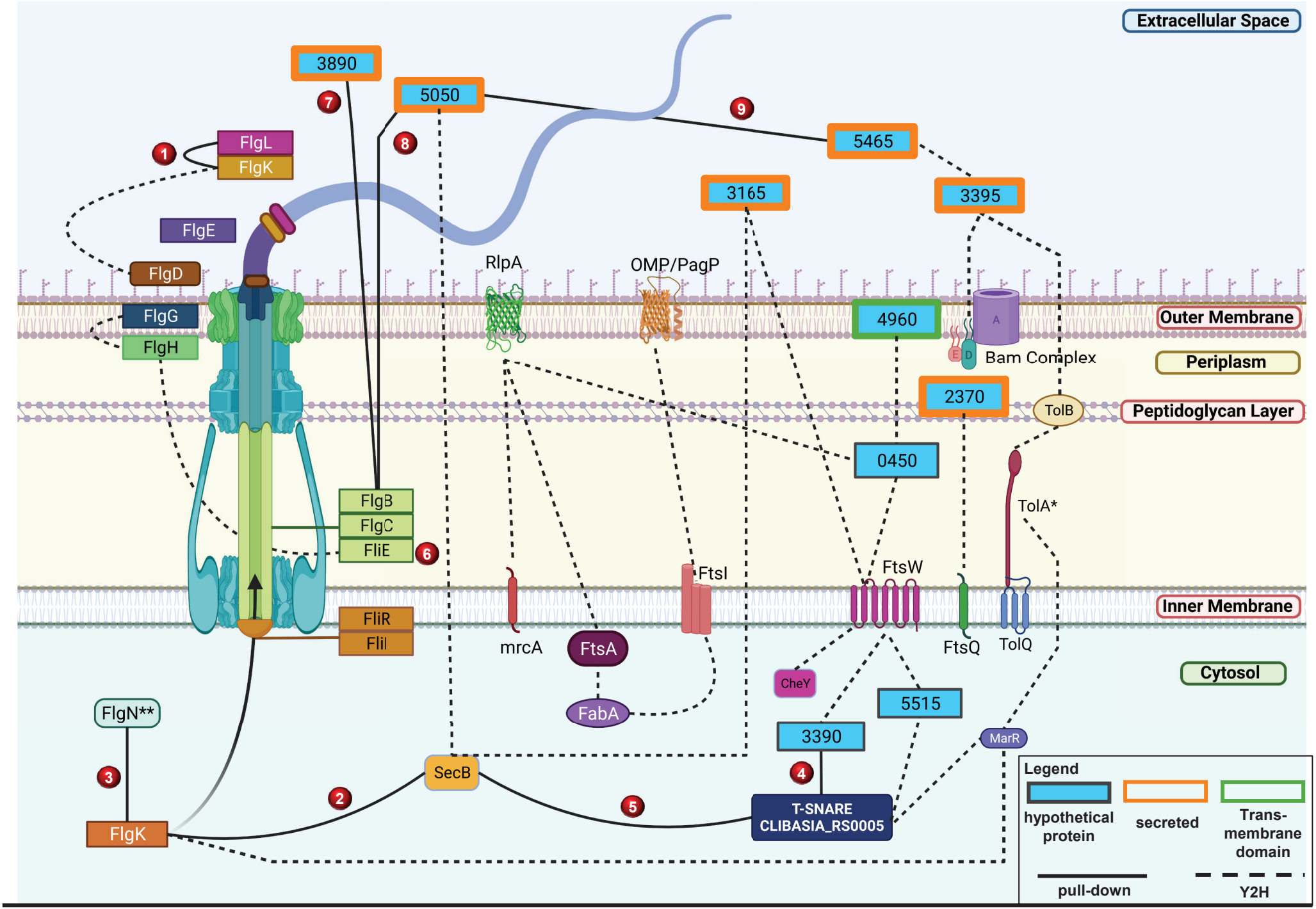

Figure 5. Integrated view of CLas proteins related to flagellar biosynthesis and membrane proteins, their interacting partners identified in Y2H. Subcellular localization representation of CLas hypothetical and annotated protein interactions. The source of the interactions and hypothetical proteins are denoted by dashed and solid lines. Hypothetical proteins with orange borders are experimentally confirmed secreted proteins as described in Prasad et al. (2016) and Du et al. (2021). Interactions confirmed with pull-down experiments were numbered from 1-9 in red circles. The hypothetical proteins were named using their CLIBASIA_RS#.

Extended Data Table S1. Previous bacterial interactome studies

Organism	Type of Organism	Total ORFs in Genome	Proteins Interacting in Y2H	% ORF Covered	Total Interactions	Avg. Number PPI per Node	System	Refference
M. loti	gram -	7277	1804	24.8	3121	1.7	ǂGal4	Shimoda et al. (DNA research, 2008)
B. subtilis	gram +	4100	287	7	793	2.8	ǂGal4	Marchadier et al. (Proteomics, 2011)
Synechocystis sp.	gram -	3692	1920	52	3236	1.7	Gal4	Sato et al. (DNA research, 2007)
E. coli	gram -	3600	1269	35.3	2234	1.8	Gal4	Uetz et al. (Nature biotechnology, 2014)
S. pneumoniae	gram +	2109	820	38.9	2045	2.5	LexA	Wuchtly et al. (ASM molecular biology and physiology, 2017)
C. jejuni	gram -	1654	1321	79.9	2884	2.2	LexA	Parrish et al. (Genome Biology, 2007)
1st *H. pylori*	gram -	1587	261	16.4	908	3.5	Gal4	Rain et al. (Nature, 2001)
2nd *H. pylori*	gram -	1587	739	46.6	1515	2.1	Gal4	Hausert et al. (Molecular and Cellular Proteomics, 2014)
"Comprehensive" *H. pylori*	gram -	1587	1135	71.5	2369	2.1	Gal4	Rain & Hausert et al. (Combined Study)
*T. pallidum**	gram -	1039	726	69.9	3649	5	Gal4	Titz et al. (PLOS One, 2008)
CLas*	gram -	1027	542	52.8	4245	7.8	Gal4	This Study
M. pneumoniae	gram +	689	617	90	10083	16.34	TAP-MS	Kuhner et al. (Science, 2009)

*Obligate intracellular; ǂ: Not a complete interactome.

Extended Data Table S2. Number of annotated and uncharacterized proteins in the CLas_whole and CLas_HC networks

Network	**Annotated**	**Uncharacterized**	**Total**
CLas_whole	371	171	542
CLas_HC	295	160	455

Extended Data Table S3. Interactions between annotated and uncharacterized proteins.

Interaction type	**CLas_whole Node**	**CLas_whole edge**	**CLas_HC node**	**CLas_HC edge**
Annotated - annotated	339	1491	246	692
Annotated - hypothetical	502	1976	388	1106
Hypothetical - hypothetical	148	570	123	388
Interologs (annotated – annotated)	128	171	96	106
Interologs (annotated – hypothetical)	47	30	30	18
Interologs (hypothetical - hypothetical)	12	7	7	4
Total	542	4245	455	2314

Extended Data Table S4. 542 CLas proteins were queried for their predicted interactions available from the STRING-db.

	STRING-db 0.4[a]		**STRING-db 0.9[b]**	
	nodes	edges	nodes	edges
All STRING association types	436	3509	256	863
Experimentally determined	115	474	81	369

Note: Two STRING datasets of experimentally proven PPIs (interaction confidence scores of ≥0.4[a] and ≥0.9[b]). The resulting network node and edge counts are listed in the table. No lab experiment datasets determined for CLas are available from STRING. All interaction associations are predicted based on experiments conducted in orthologs.

Extended Data Table S5. Count of uncharacterized proteins by each annotation evidence/method used.

Annotation Method	Number of uncharacterized proteins
protein families' association	39
metainteractome	16
operon association	12
protein families' association; operon association	11
PPI	7
metainteractome; protein families association	6
PPI; structure	4
metainteractome; operon association	2
protein families' association; PPI	1
protein families' association; structure	1
metainteractome; PPI	1
metainteractome; protein families association; PPI	1
Total	101

Extended Data Table S6. PPIs between 22 flagellar proteins in the CLas Y2H.

Interaction type	CLas_whole Node	CLas_whole edge	CLas_HC node	CLas_HC edge
annotated Flg proteins – all PPIs	213	399	118	175
annotated Flg proteins – annotated protein	122	240	59	103
annotated Flg proteins – uncharacterized	69	151	40	67
annotated Flg proteins – annotated Flg proteins	9	8	7	5

Extended Data Table S7. CLas PPIs involving flagellar and membrane proteins.

Protein names	Interacting proteins	Interaction
CLIBASIA_RS01145	CLIBASIA_RS00005	Y2H
CLIBASIA_RS01945	CLIBASIA_RS00005	confirmed by pull down
CLIBASIA_RS01945	CLIBASIA_RS00005	Y2H
CLIBASIA_RS03390	CLIBASIA_RS00005	confirmed by pull down
CLIBASIA_RS03390	CLIBASIA_RS00005	Y2H
CLIBASIA_RS01945	CLIBASIA_RS03165	Y2H
CLIBASIA_RS03290	CLIBASIA_RS03395	Y2H
CLIBASIA_RS01290	CLIBASIA_RS03890	confirmed by pull down
CLIBASIA_RS01290	CLIBASIA_RS03890	Y2H
CLIBASIA_RS01290	CLIBASIA_RS05050	confirmed by pull down
CLIBASIA_RS01290	CLIBASIA_RS05050	Y2H
CLIBASIA_RS01945	CLIBASIA_RS05050	Y2H
CLIBASIA_RS03395	CLIBASIA_RS05245	Y2H
CLIBASIA_RS04925	CLIBASIA_RS01685	Y2H
CLIBASIA_RS05260	CLIBASIA_RS01685	Y2H
CLIBASIA_RS03410	CLIBASIA_RS03430	Y2H
CLIBASIA_RS01255	CLIBASIA_RS01275	Y2H
CLIBASIA_RS01945	CLIBASIA_RS03410	confirmed by pull down
CLIBASIA_RS03415	CLIBASIA_RS03410	confirmed by pull down
CLIBASIA_RS03480	CLIBASIA_RS03410	Y2H
CLIBASIA_RS03480	CLIBASIA_RS03415	Y2H

CLIBASIA_RS01230	CLIBASIA_RS01280	confirmed by pull down
CLIBASIA_RS01230	CLIBASIA_RS01280	Y2H
CLIBASIA_RS01255	CLIBASIA_RS01280	Y2H
CLIBASIA_RS01290	CLIBASIA_RS01280	Y2H
CLIBASIA_RS02290	CLIBASIA_RS04130	Y2H
CLIBASIA_RS05260	CLIBASIA_RS04130	Y2H
CLIBASIA_RS03410	CLIBASIA_RS03480	confirmed by pull down
CLIBASIA_RS03410	CLIBASIA_RS03915	Y2H
CLIBASIA_RS04130	CLIBASIA_RS00450	Y2H
CLIBASIA_RS04900	CLIBASIA_RS00450	Y2H
CLIBASIA_RS04900	CLIBASIA_RS03165	Y2H
CLIBASIA_RS04900	CLIBASIA_RS03915	Y2H
CLIBASIA_RS04900	CLIBASIA_RS05515	Y2H
CLIBASIA_RS04960	CLIBASIA_RS00450	Y2H
CLIBASIA_RS05050	CLIBASIA_RS05465	confirmed by pull down
CLIBASIA_RS05265	CLIBASIA_RS02370	Y2H
CLIBASIA_RS05465	CLIBASIA_RS03395	Y2H
CLIBASIA_RS05515	CLIBASIA_RS00005	Y2H

Extended Data Table S8. CLas protein-protein interactions that were confirmed by pull-down assay

CLas Locus id	CLas protein molecular weight (kDa)	protein + GST VECTOR (kDa)	protein + MBP VECTOR (kDa)	NCBI Annotation
CLIBASIA_RS00005	14.4	40.4	56.4	hypothetical protein
CLIBASIA_RS01230	34.5	60.5	na	FixB
CLIBASIA_RS01280	11.7	na	53.7	FliE
CLIBASIA_RS01290	14.6	Na	56.6	FlgB
CLIBASIA_RS01945	17.4	43.4	59.4	SecB
CLIBASIA_RS03390	45.8	Na	87.8	chemotaxis protein
CLIBASIA_RS03410	53.9	79.9	na	FlgK
CLIBASIA_RS03415	40.2	Na	82.2	FlgL
CLIBASIA_RS03480	13.9	Na	55.9	hypothetical protein (putative FlgN)
CLIBASIA_RS03890	9.4	35.4	na	hypothetical protein
CLIBASIA_RS05050	11.2	37.2	na	hypothetical protein
CLIBASIA_RS05465	7.4	Na	49.4	hypothetical protein

A)

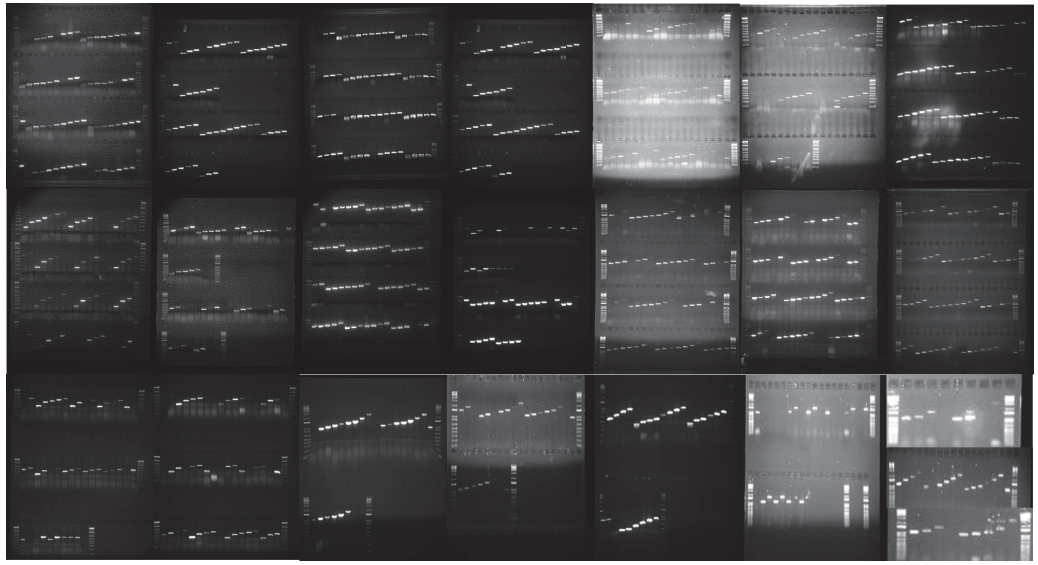

B)

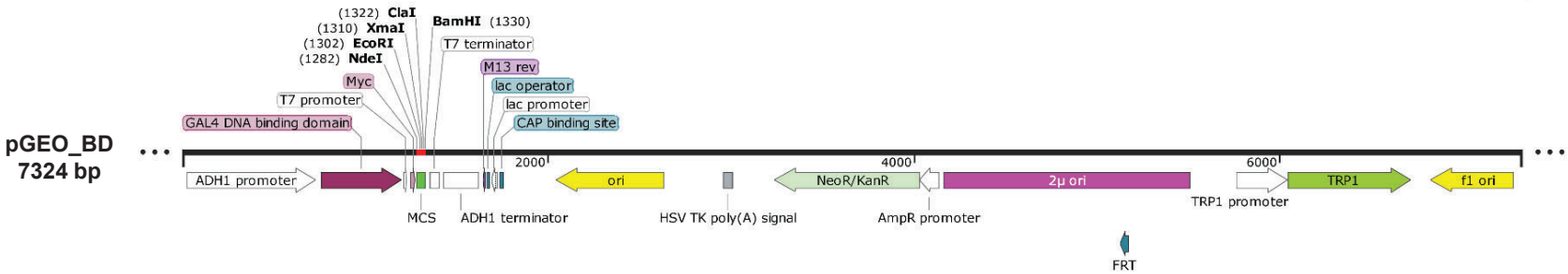

Extended Data Figure S1. Cloning of CLas genes for Y2H. A) Amplification of CLas ORFs for infusion cloning. Primers for 1027 CLas ORFs were designed, resulting in 974 successfully amplified genes for Y2H high throughput interaction screening. **B) Modification of Yeast Two-Hybrid expression vectors enables efficient cloning of all CLas ORFs into two vectors.** A fragment containing the pGADT7 AD (clonetech) MCS sequence between NdeI and BamHI was used to replace the MCS in pGBKT7 (clonetech) between the restriction sites NdeI and BamHI to create a new binding domain vector pGEO_BD. The modified MCS allowed us to design only one primer set for each CLas gene to clone into both AD and BD vectors using Infusion cloning (Clonetech) for the Y2H high-throughput screening. MCS: multiple cloning site.

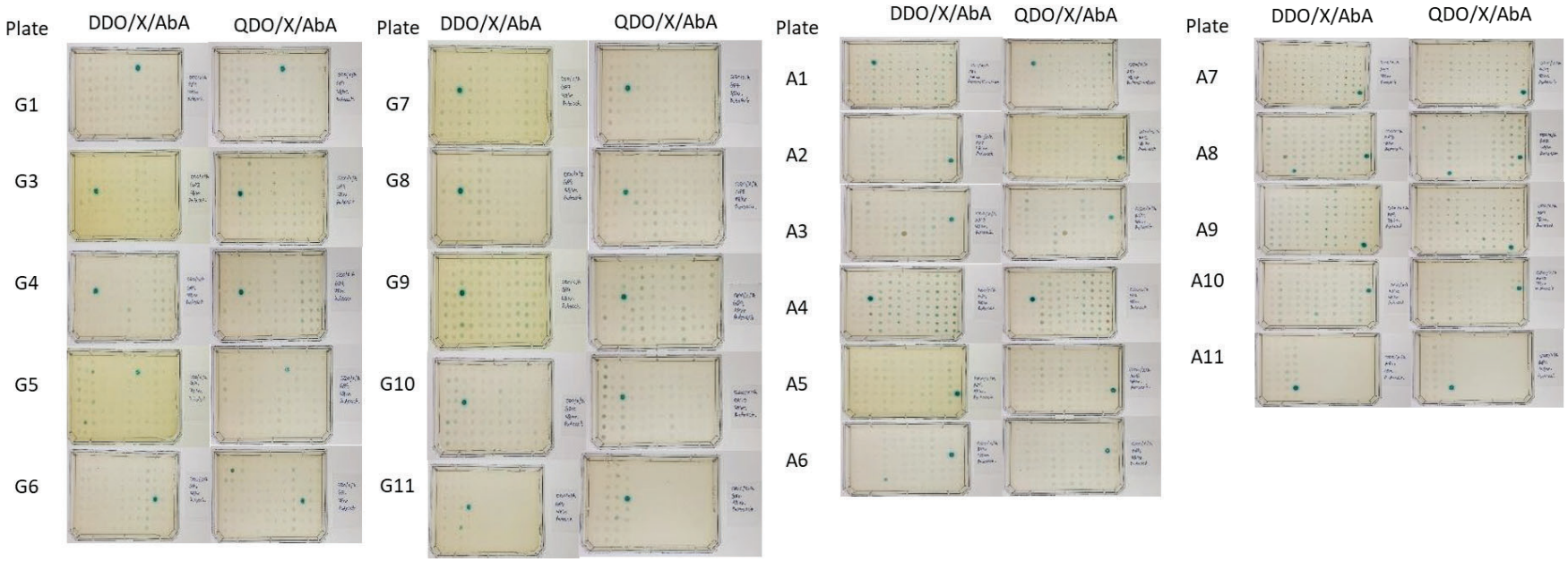

Extended Data Figure S2. Constructing and testing yeast expression vectors. Autoactivation screening for CLas ORF constructs in both AD and BD vectors. From the ORFs cloned into both the AD and BD Y2H vectors, constructs were transformed into Mat-a yeast and mated with Mat-α yeast harboring the empty vector opposite of the construct; i.e., AD construct mated with BD empty vector, vice versa.

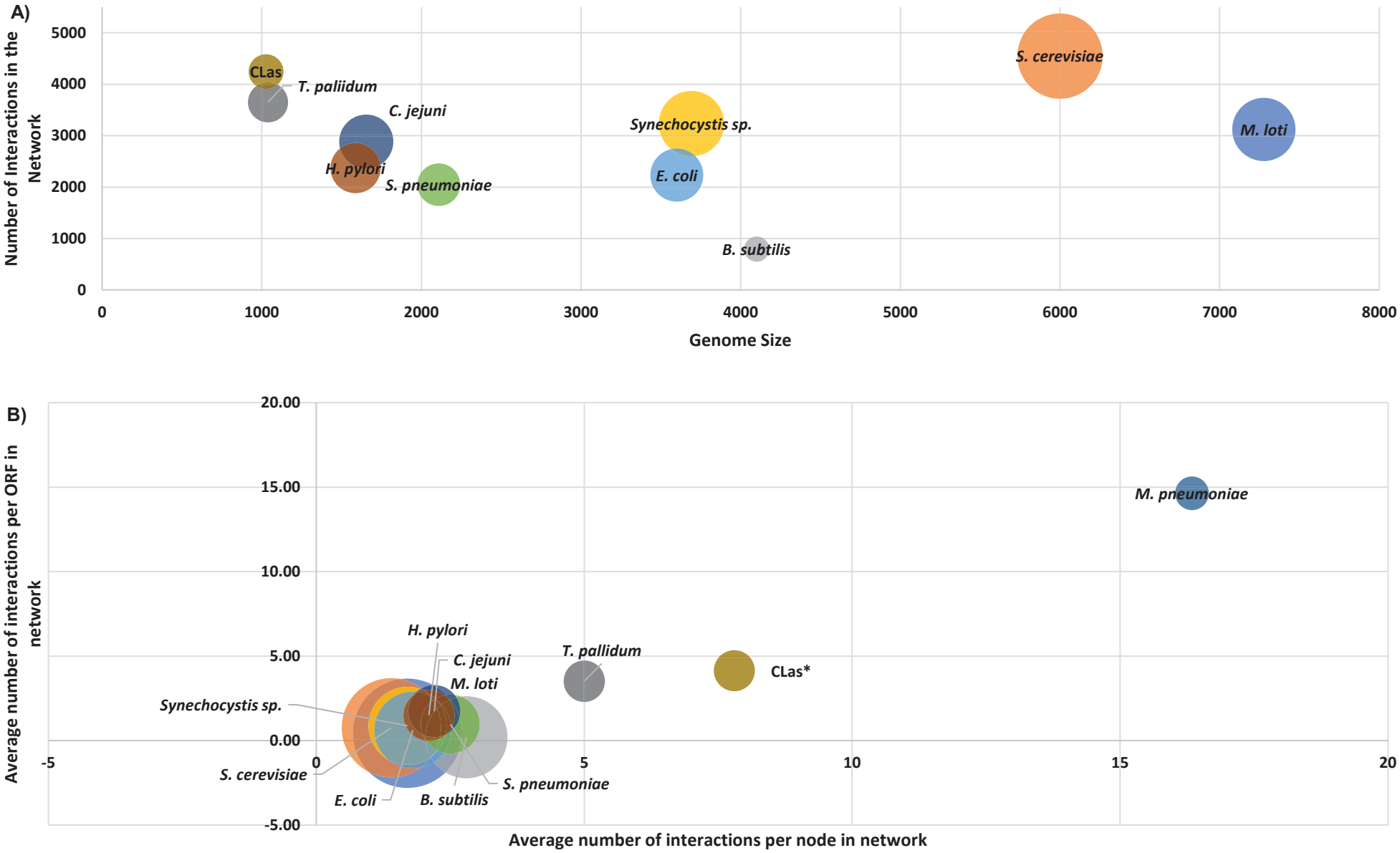

Extended Data Figure S3. Comparison of CLas interactome with other bacteria. A. Two interactomes of bacteria with reduced genome sizes (CLas and *T. pallidum*) have a higher number of interactions between fewer number of proteins, compared to other interactomes. Here, the genome size, number of nodes, and number of interactions were compared across nine interactomes. Bubble size represents number of nodes in a network. **B.** Relationship between genome size and the average number of interactions per node. The CLas_whole is shown in comparison to other interactomes. Bubble size represents genome size.

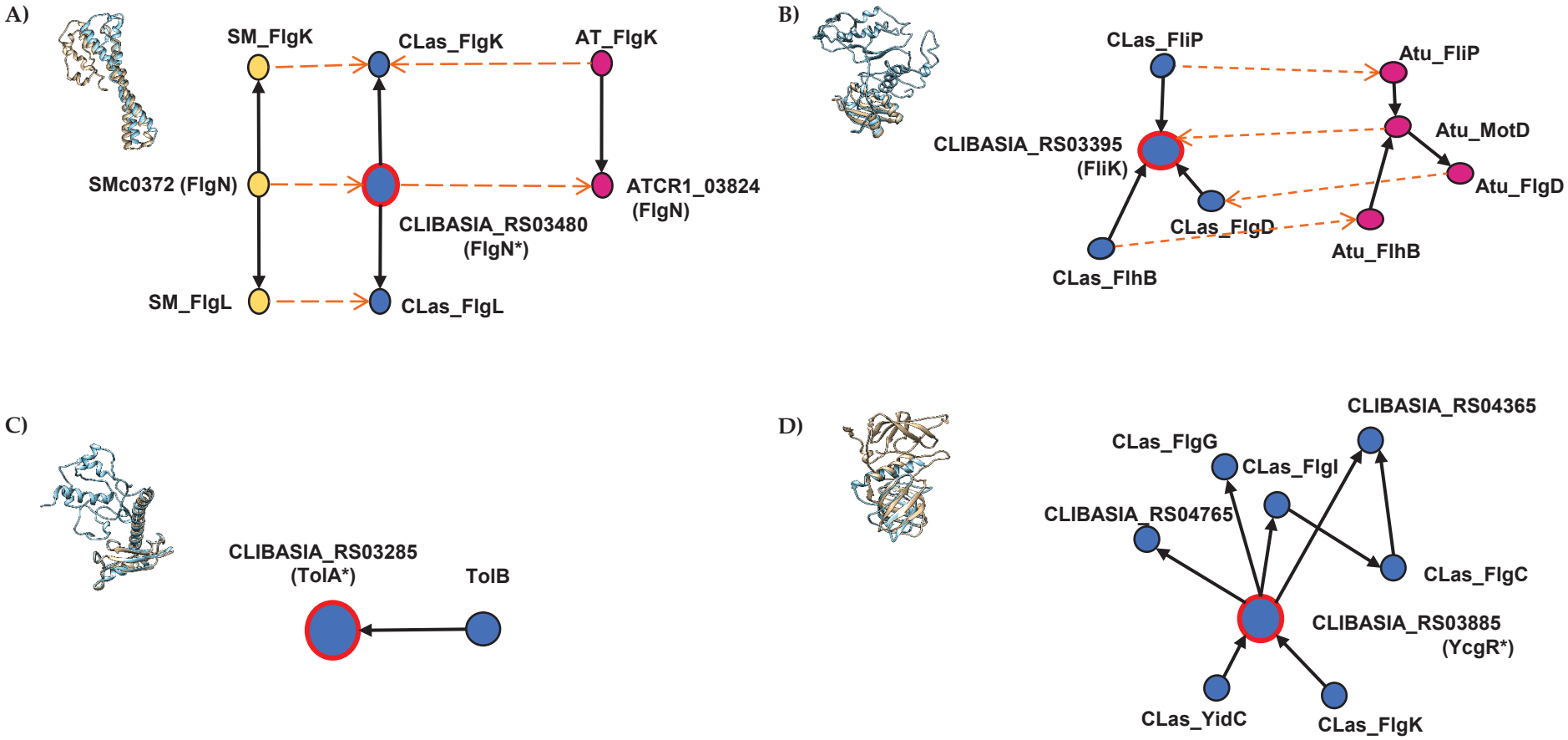

	Locus ID	CLas uncharacterized protein NCBI annotation	annotation this study	structure identity (%)	confidence score (100)	AA sequence identity (%)	AA query cover (%)
A	CLIBASIA_RS3480	hypothetical protein	FlgN	17.89	83.2	31	79
B	CLIBASIA_RS3395	hypothetical protein; putative MotD	FliK	68.83	90.2	36.11	18
C	CLIBASIA_RS3285	hypothetical protein	TolA	45.63	100	35.05	35
D	CLIBASIA_RS4365	PilZ domain-containing protein	YcgR	25	98	25.93	11

Extended Data Figure S4. Protein-protein interactions, interologs, and protein structure homology data were used to assign putative functions for CLas uncharacterized proteins. The Phyre2 online database was used to predict CLas protein structures and find possible template matches of HMM homolog proteins and characterized proteins. Protein structure alignments of CLas proteins (blue), aligned and superimposed over protein Phyre2 protein templates (gold). Alignment and confidence data for each are shown below the figures**. A)** Protein structure alignment of CLIBASIA_RS03480 and *Bradythizobium* FlgN. The interologs in *S. meliloti* (yellow) and *A. tumefaciens* (purple) suggest that CLIBASIA_RS03480 To be FlgN. **B)** CLIBASIA_RS3395 was annotated to be FliK based on structure alignment and interologs in *A. bacterium*. **C)** CLIBASIA_RS3285 was annotated to be TolA based on structure alignment and its interaction with CLas TolB in the Y2H network. **D)** CLIBASIA_RS4365 was annotated to be YcgR flagellar brake protein based on structure alignment and interacting partners in Y2H. * annotation was conducted in this study.

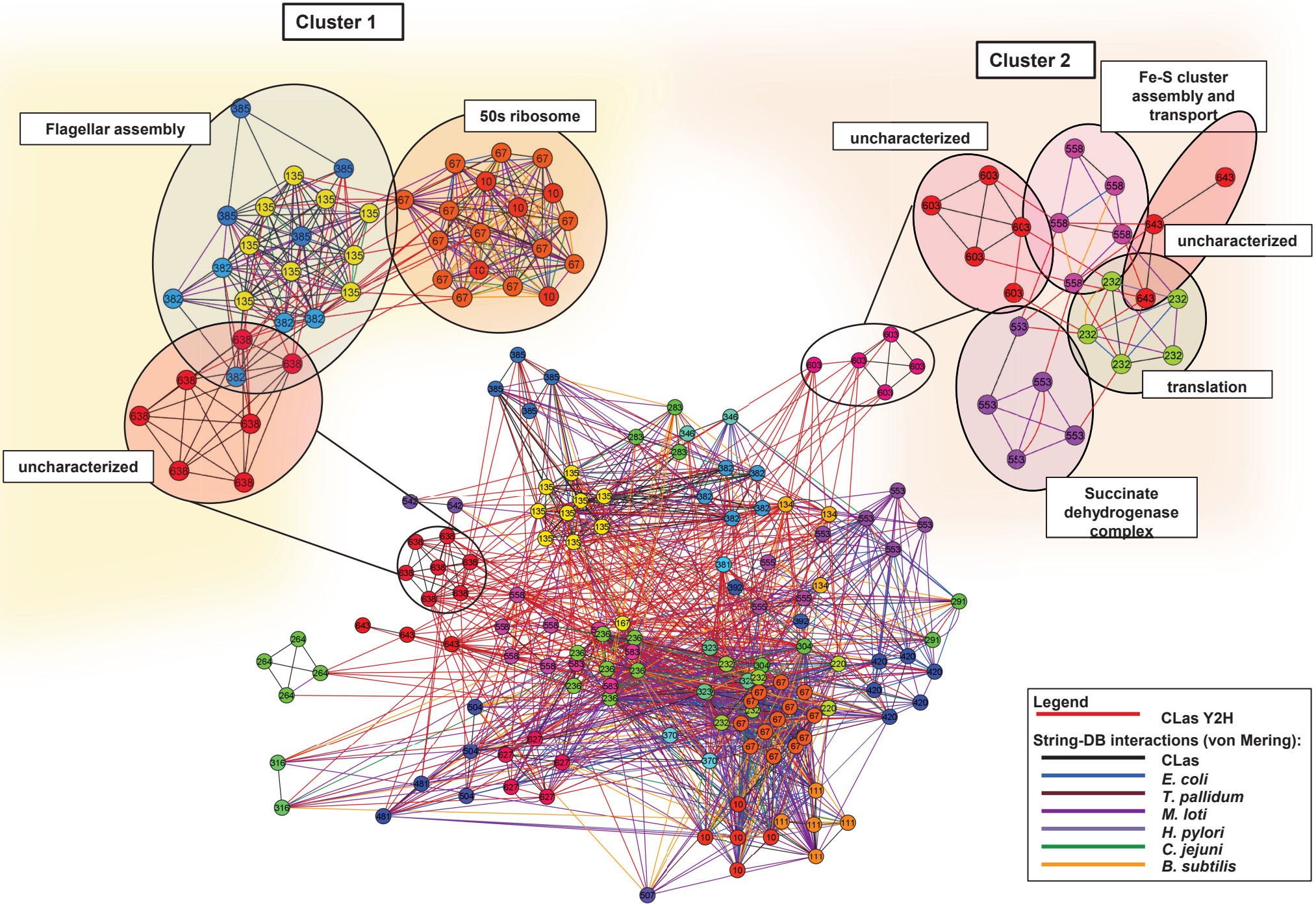

Extended Data Figure S5. Inter-operon interactions highlight associations between motility related genes, respiration, membrane integrity, ribosomal proteins, and uncharacterized genes and operons. The large network shown below the two subnetwork clusters is the CLas operon network. Operons were predicted using the ProOpDB: Prokaryotic Operon Data Base (http://operons.ibt.unam.mx/OperonPredictor). CLas operons with ≥2 PPIs with another operon are shown. Three operonic gene clusters of uncharacterized proteins interact with annotated CLas proteins; uncharacterized operons are in red; i.e.: 603, 638, and 643. Edges are colored by PPI source. The CLas Y2H PPIs in this study are represented by red edges.

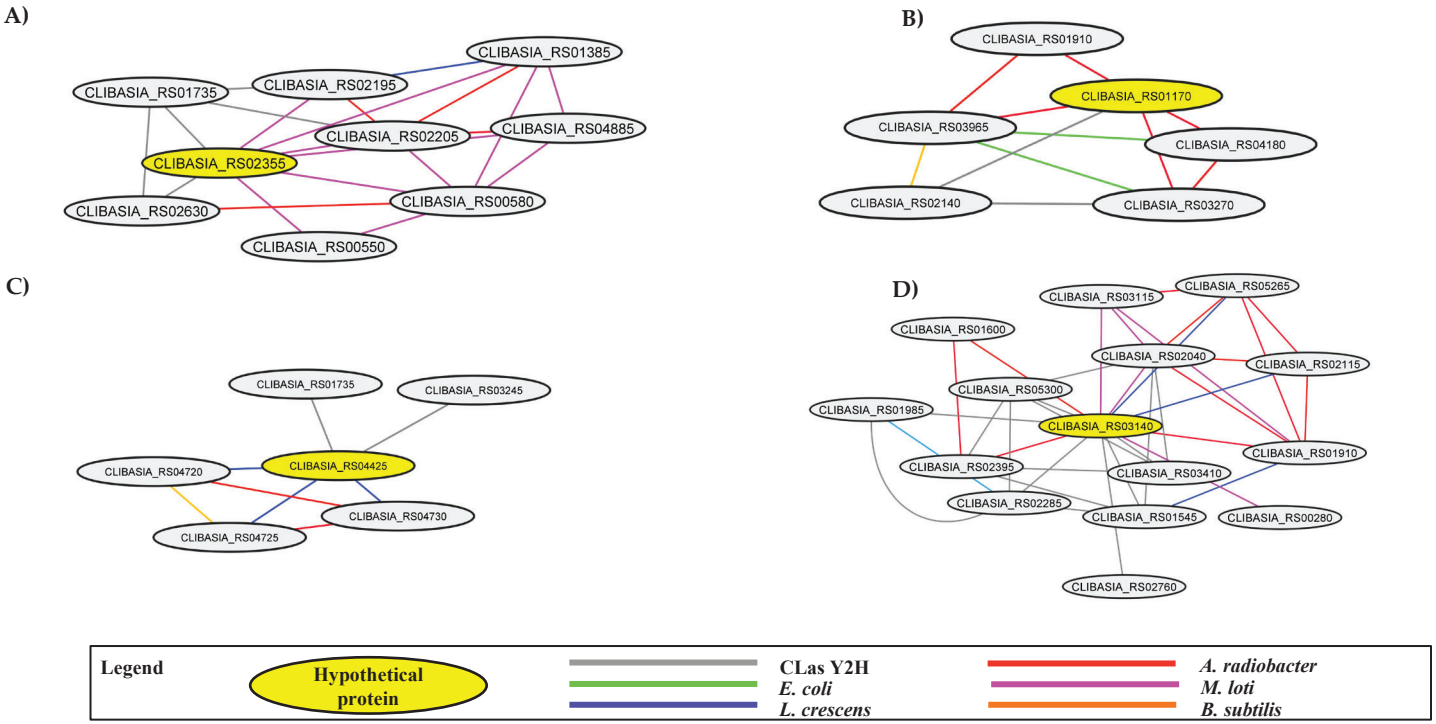

Extended Data Figure S6 Meta-interactome subnetworks. Four hypothetical proteins whose protein function was inferred by its ortholog associations found in meta-interactome (mY2H) subnetworks. Edges are colored by ortholog PPI. A. CLIBASIA_RS02355 has a putative association with cell wall formation and lipid synthesis. B. CLIBASIA_RS04425 has a putative association with FeS cluster assembly, DNA YacG, and RNA pyro phosphohydrolase. C. CLIBASIA_RS0170 has a putative association with DNA processing related proteins. D. CLIBASIA_RS03140 has a putative association with cell division.